Journal of Materials Chemistry B

REVIEW

View Article Online
View Journal | View Issue

Cite this: J. Mater. Chem. B, 2025, 13, 12812

Advancements in anterior cruciate ligament reconstruction based on weaving technology: current developments and future prospects

Danjie Yang, [a] Faqian Shen [b] and Xiaogang Chen *[a]

Anterior cruciate ligament (ACL) reconstruction is a crucial surgical approach for rapidly restoring the function of an injured knee. Earlier approaches focused on repair techniques that often did not aim to replicate the native anatomy and function of the tissue (non-anatomical). In contrast, the field has shifted towards anatomic reconstruction methods, which prioritise restoring the native structure and biomechanics using autografts or synthetic materials. Textile technologies, especially weaving, have gained great attention for their capacity to create complex structures with the desired properties for various applications. By adjusting key parameters such as fibre arrangement, weave pattern, fibre/yarn linear density and warp/weft density, woven-based grafts can replicate the hierarchical structure, bioinspired morphology, anisotropic characteristics and mechanical properties of natural human tissues. This review examines the materials, structural designs, and functional outcomes of textile-based strategies for ACL reconstruction, with a particular focus on weaving technology. Key challenges for clinical translation are discussed, and future directions are explored. Weaving technology is highlighted as a promising strategy to address current limitations and guide future developments in ACL graft design.

Received 23rd March 2025,
Accepted 4th September 2025

DOI: 10.1039/d5tb00669d

rsc.li/materials-b

1. Introduction

The ACL is a highly specialised connective tissue crucial for transmitting forces from bone to bone, thereby facilitating joint movement and bodily motion. The structures of the ACL possess physiological limits concerning their capacity to withstand forces, exceeding which can result in ACL damage, leading to joint pain and compromised bodily function.[1] Injuries to the ACL are frequent in sports activities, often resulting from exposure to substantial forces, such as sudden changes in movement direction, rapid stops, abnormal jumping and landing, a direct hit on the outside of the knee, or deceleration while running.[2] These injuries are regarded as severe forms of ligament damage, resulting in significant structural and functional impairment of the knee joint.[3] Due to their high prevalence, they are among the most common musculoskeletal diseases in clinical practice.[4] The United States records 33 million musculoskeletal injuries annually, nearly half of which are related to ligament injuries.[5,6] While most injuries are not critical, they can lead to severe disability, significantly reduce a patient's quality of life, decrease productivity and lead to significant healthcare costs.[7] A significant increase was witnessed in reported ligament tear cases in the past ten years, with the mean age of affected individuals being 30 years old in the United Kingdom during this period.[8,9] As the ACL is crucial for maintaining proper knee movement and joint stability, its absence can cause joint instability, increasing the risk of secondary damage to the menisci and articular cartilage, which results in early-onset osteoarthritis.[10,11] Unfortunately, owing to low cellularity and insufficient blood supply, the ACL has minimal ability to regenerate itself[12–14] and often requires surgical treatment for repair.

ACL injuries are usually classified into three grades according to the extent of anterior tibial displacement.[15,16] Grade I injuries involve damage to less than one-third of the ligament and are usually asymptomatic. Grade II and grade III injuries are more severe and usually present with symptoms such as knee dysfunction and tenderness. In the surgical treatment of ACL injuries, there are generally two main approaches: enhancing primary repair and graft-based reconstruction.[17–19] The primary repair approach aims to restore the torn ACL by guiding and supporting the repair with sutures or scaffolds, retaining the native ACL and its proprioceptive nerves. Although this approach is attractive due to the preservation of the native tissue, its effectiveness is limited by the ACL's low vascularity and cellularity, which hinders long-term healing and regeneration.[20–24] Despite various enhancement methods being explored to promote cellular proliferation and migration

[a] Department of Materials, University of Manchester, Manchester, UK. E-mail: Xiaogang.chen@manchester.ac.uk
[b] School of Life Science, Nanjing University, Nanjing, China

into the scaffold, the results are often insufficient for complete recovery.[25–27] Consequently, the majority of orthopaedic surgeons opt for graft-based ACL reconstruction. This technique involves removing the damaged ACL and drilling tunnels into the bone at the original ACL attachment sites. A graft is then inserted into these tunnels and anchored in place. One of the key advantages of graft-based reconstruction is the immediate restoration of mechanical function in the knee after surgery. However, an obvious challenge associated with this approach is that the desired ACL graft must be able to faithfully replicate the complex structural, compositional and functional attributes of the native ACL to be consistently effective as a long-term replacement within the knee joint.

Surgical reconstruction is often necessary to restore knee function, especially for active individuals. The current clinical gold standard involves using biological grafts, either autografts (tissue harvested from the patient's own body, such as patellar tendons or hamstring tendons) or allografts (tissue from a deceased donor).[28] While these approaches have achieved considerable success, they are not without significant drawbacks. Autografts are associated with donor site morbidity, including pain, numbness, and weakness at the harvest site.[29,30] The availability of suitable autograft tissue is also limited. Allografts, while avoiding donor site morbidity, introduce risks of disease transmission and can elicit an immunogenic response in the host.[31] Furthermore, both autografts and allografts undergo a period of remodelling and revascularization *in vivo*, during which their mechanical properties are significantly reduced, increasing the risk of re-rupture.[32] The initial mechanical properties of these grafts often do not perfectly match those of the native ACL, leading to potential long-term joint instability or altered kinematics.[33] These limitations have created a clear clinical need for an off-the-shelf, biocompatible, and mechanically robust alternative.

In recent years, textile technologies, such as weaving, braiding, knitting and electrospinning, have been used to manufacture fibrous scaffolds in a range of tissue-engineering applications.[34–39] Woven structures allow for precise control over parameters such as fibre orientation, pore size, porosity and surface morphology. These parameters play crucial roles in determining the physical characteristics and cellular responses of engineered grafts. An overview of these different graft types and materials along with key scaffold features is presented in Fig. 1.

This review provides a critical analysis of the design, fabrication, and performance of woven scaffolds for ACL reconstruction. It aims to review the current state of knowledge, evaluate weaving against alternative techniques, and identify key challenges and future directions. The ultimate goal is to present a comprehensive overview of how weaving technology can address the limitations of current ACL treatments.

2. Literature review methodology

To conduct a comprehensive review of advancements in ACL reconstruction based on weaving technology, we employed a systematic literature search strategy. This strategy focused on identifying and analysing relevant scientific literature accessible through established databases such as PubMed, Scopus and Google Scholar. The objective was to gather insights into the application of weaving technology in ACL reconstruction methodologies, including the fabrication of biomimetic scaffolds, their mechanical properties, biocompatibility, degradation profiles, and clinical translation potential.

The search criteria were divided into three primary sections:

1. Keywords related to textile technology: we used terms such as "woven," "weaving," "textile," "fabric," and "scaffold" to capture the range of textile techniques, with a primary focus on weaving, applied in ligament tissue engineering. While other textile techniques like "braiding," "knitting," and "electrospinning" were also considered in broader initial searches to

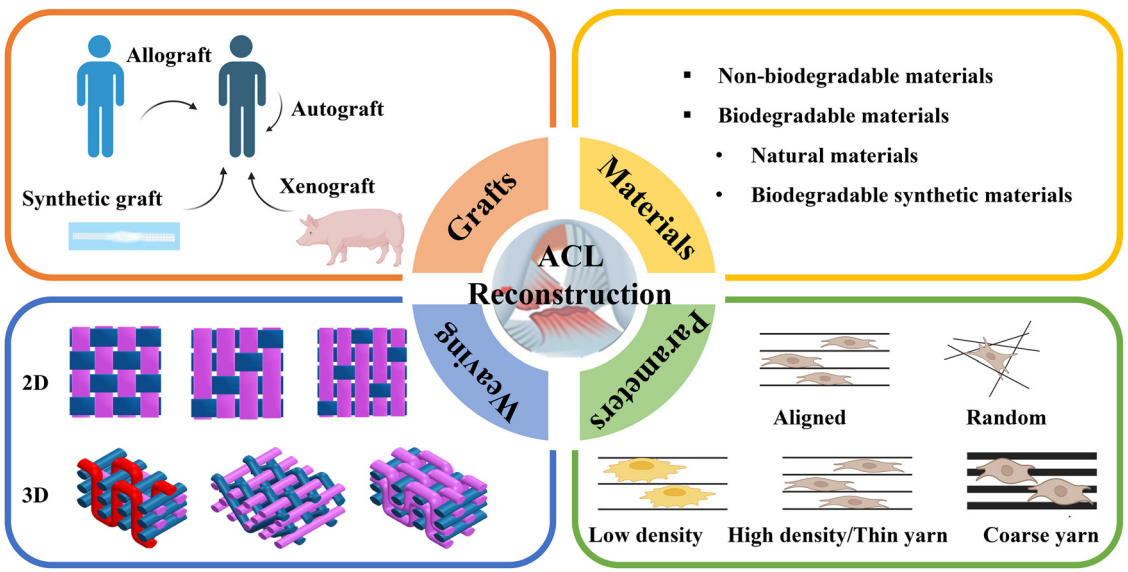

Fig. 1 Overview of different graft types and materials used in ACL reconstruction, along with key scaffold features important for tissue engineering.

provide context for comparative analysis, the core focus remained on woven structures.

2. Terminology for ACL applications: this included specific terms like ''anterior cruciate ligament,'' ''ACL,'' ''reconstruction,'' ''repair,'' and ''regeneration'' to ensure the search was directly relevant to ACL tissue engineering and therapeutic devices.

3. Application-specific terminology: keywords such as ''biomimetic scaffolds,'' ''biocompatibility,'' ''mechanical properties,'' ''cell proliferation,'' ''tissue engineering,'' ''degradation,'' ''clinical trial,'' and ''translational'' were used to identify studies focusing on the functional and structural integration of textile-based constructs in ACL therapies, as well as their progression towards clinical use.

To enhance the rigor of our research, we implemented specific inclusion and exclusion criteria.

Inclusion criteria: (1) peer-reviewed original research articles and comprehensive review articles published in English between 2015 onwards to ensure contemporary relevance. (2) Studies explicitly focusing on the application of woven textile technologies in ACL reconstruction or regeneration. (3) Research presenting original experimental data, including *in vitro*, *in vivo* (animal models), or human clinical studies. (4) Articles discussing key aspects such as mechanical properties, biological safety, cellular interactions, degradation kinetics, and clinical outcomes of woven ACL scaffolds.

Exclusion criteria: (1) articles not directly related to ACL reconstruction or woven textile fabrication techniques for musculoskeletal applications. (2) Studies without accessible full texts. (3) Publications focusing on non-ACL applications of textile technologies or general textile engineering not specifically applied to ligament/tendon tissue engineering and repair. (4) Conference abstracts, dissertations, book chapters, or non-peer-reviewed publications, unless they were foundational works widely cited in the peer-reviewed literature.

Data extraction involved systematically collecting information on study objectives, the specific woven textile fabrication techniques employed, materials used, detailed experimental designs (including *in vitro* and *in vivo* models), key findings, and conclusions. We also noted details regarding control setups, statistical methods employed, and assessments of reproducibility to evaluate the quality and reliability of the studies.

Data synthesis involved categorizing the identified studies primarily based on the specific woven textile techniques and their application within ACL reconstruction. We meticulously analysed the reported mechanical properties (*e.g.*, tensile strength, strain, and stiffness), biocompatibility (*e.g.*, inflammatory response and foreign body reaction), cellular responses (*e.g.*, cell adhesion and proliferation), and degradation profiles (*e.g.*, mass loss, molecular weight changes, and correlation with tissue ingrowth). Statistical analyses presented within the studies were critically examined to assess the significance and robustness of the findings. By integrating these diverse datasets, we aim to provide a comprehensive overview of how weaving technologies are advancing ACL reconstruction therapies, highlighting both the potentials and limitations observed in the current literature.

3. Materials in ACL reconstruction

The choice of the ACL scaffold material is closely related to the intended treatment plan. While all such interventions are classified as ACL reconstruction, current clinical strategies fall into two main categories: permanent ligament replacement and biologically guided regeneration.[40] Replacement approaches employ non-degradable, mechanically strong materials designed to replace the native ligament and provide long-term or permanent mechanical function.[41] Regenerative strategies, on the other hand, utilise biodegradable, biocompatible materials designed to offer temporary mechanical support while promoting endogenous cell infiltration, tissue remodelling and neo-tissue formation.[42] These diverse approaches impose distinct design criteria on scaffold materials and are associated with differing clinical benefits and translational challenges.

3.1. Non-degradable materials for permanent replacement

The earliest synthetic ligaments were designed for permanent replacement, aiming to provide immediate and lasting mechanical stability. The primary materials used for this purpose are non-biodegradable polymers, chosen for their high strength and durability.[41] Polyethylene terephthalate (PET) is the most common of these materials, famously used in the ligament augmentation and reconstruction system (LARS) and the Leeds–Keio ligament. PET-based grafts exhibit excellent mechanical properties immediately after implantation.[43] Short- to mid-term clinical outcomes were favourable. For example, Batty *et al.*[44] reported that the LARS had the lowest failure rate (2.6%) among synthetic grafts, despite relatively limited follow-up. Similarly, Ebert and Annear[45] observed promising results with hamstring autografts augmented with the LARS ligament at 2 years of follow-up, with only 1 graft failure in 50 patients.

However, the long-term clinical performance was unsatisfactory. Despite high initial strength, long-term cyclic loading can lead to fatigue failure and graft rupture, with long-term studies reporting failure rates as high as 24–50%.[46,47] This mechanical instability is often accompanied by a detrimental biological response, wherein the generation of wear debris induces a chronic inflammatory response (synovitis), leading to pain and progressive joint degeneration. Indeed, long-term follow-up studies have reported synovitis rates as high as 58%, reoperation rates of 51%, and histological confirmation of a foreign body reaction characterized by giant cells.[47,48] Furthermore, as permanent implants, these grafts fail to integrate with the host tissue. Their high stiffness protects the surrounding bone from physiological stress, leading to bone resorption and tunnel widening. This chain reaction of mechanical failure, chronic inflammation and poor integration is believed to be the primary cause of the high incidence of postoperative osteoarthritis, reported in one 10-year follow-up study as high as 63%.[46] As highlighted by Huang *et al.*[49] maximising mechanical strength beyond physiological levels can lead to severe mechanical mismatch, ultimately leading to stress shielding and compromised joint biomechanics. These observations reveal fundamental limitations of permanent replacements,

leading to a growing shift away from permanent replacements and toward strategies that promote biological regeneration.

3.2. Biodegradable materials for guided regeneration

The philosophy behind guided regeneration is to use a temporary scaffold that provides initial mechanical support but is gradually replaced by newly formed, functional ligament tissue.[50] This approach prioritises biocompatibility and bioactivity, aiming to harness the body's own healing capacity.

Biodegradable materials such as collagen,[51] silk,[52,53] polycaprolactone (PCL),[54] polydioxanone (PDO),[55] polyglycolic acid (PGA),[56] poly(L-lactic) acid (PLLA)[57] and poly(lactic-*co*-glycolic) acid (PLGA)[58] are considered promising candidates for ligament grafts. Studies on these materials have shown positive results regarding cell attachment, infiltration and ECM production.[57,59,60] However, this strategy faces three major challenges: the trade-off between mechanical strength and biological safety, the control of degradation kinetics, and the management of the host immune response.[61]

Scaffolds made purely from biodegradable polymers often suffer from insufficient initial mechanical strength; for example, ultra-high molecular weight polycaprolactone (UHMWPCL) grafts can achieve only 41.9% of the ultimate load of the native ACL *in vivo*.[62] This has led to the development of composite or hybrid materials. For instance, designs combining silk and collagen have exhibited excellent biological performance, but their mechanical properties remain substantially lower than the native ACL.[63]

Successful design of regenerative scaffolds requires that their degradation properties be perfectly synchronised with tissue formation.[64] This rate mismatch is a major cause of failure. If degradation occurs too rapidly, the construct may mechanically fail before the new ligament becomes robust. Conversely, slow degradation results in long-term stress shielding. In this context, ideal degradation profiles for ACL scaffolds should preserve mechanical integrity for several weeks or months, corresponding to the early proliferative and matrix deposition phases of ligament healing, followed by a controlled resorption phase aligned with native tissue remodeling.[65] The degradation kinetics are determined by material choice (*e.g.*, rapid hydrolysis of PGA *vs.* slow degradation of PCL) and can be structurally controlled through weaving, as demonstrated by Xie *et al.*,[66] who used a gradient of fast- and slow-degrading yarns to create channels for cell infiltration while maintaining a stable core. A more sophisticated approach was proposed by Li *et al.*[67] using a tri-component yarn with a strong PET core sheathed in a biodegradable polymer, an intelligent strategy to bridge the gap between initial strength and long-term biointegration. Moreover, recent studies highlight the importance of modelling scaffold degradation kinetics to better predict and optimise long-term scaffold performance. Computational models that include hydrolytic degradation,[68] enzyme activity,[69] mechanical loading,[70] and tissue ingrowth dynamics[71] can provide valuable insights into the link between degradation and regeneration, and guide the rational design of woven scaffolds with spatially and temporally controlled properties.

Finally, the implantation of any biomaterial inevitably incites a foreign body reaction. The goal is to minimise this response and resolves into a pro-regenerative (M2 macrophage) state rather than chronic inflammation. The acidic byproducts produced by polyester degradation can trigger this inflammatory response, but material selection and design can mitigate this. Cai *et al.*[72] demonstrated that their silk-PLLA hybrid woven scaffold could actively modulate macrophages towards the favourable M2 phenotype, suggesting that advanced scaffolds can be designed not only to be inert, but also to actively guide positive immune and healing response. To build on these insights, future research should include long-term *in vivo* immune analysis and biocompatibility studies to guide scaffold development.

4. Comparative analysis: weaving *vs.* alternative textile techniques

Textile technologies offer promising methods for creating biomimetic ligament implants that behave like native ACLs, including braiding,[49,73–75] knitting,[63,67,76] electrospinning and weaving.[77] While this review focuses primarily on weaving, a critical comparison with other fabrication methods is essential to realise their advantages and limitations. The optimal technique for ACL scaffold engineering is one that provides the best balance of mechanical strength, structural biomimicry and biological functionality.

The primary function of an ACL scaffold is to provide immediate knee stability. Therefore, its mechanical properties, particularly tensile strength, stiffness, strain and Young's modulus, are significant. Table 1 provides a benchmark comparison of properties achieved using different materials and techniques. To properly evaluate the performance of engineered scaffolds, it is essential to define and consistently apply key biomechanical terms. Ultimate tensile strength refers to the maximum stress a material can withstand when stretched or pulled before breaking. Stiffness is a measure of an elastomer's ability to resist deformation by an applied force. In a tensile test, it is the slope of the linear portion of the load–displacement curve. The modulus, or Young's modulus, is an intrinsic property of a material that measures its stiffness and is defined as the ratio of stress to strain in the elastic region. Strain is the percentage increase in length of a material when subjected to tensile stress. Finally, in textiles, linear density (usually measured in tex or denier) refers to the mass per unit length of a fibre or yarn, which is a key parameter influencing the ultimate mechanical properties of the scaffold.

Successful regeneration requires scaffolds that not only bear load but also actively guide tissue formation. Here, structural differences are critical. Table 2 provides a comparison of biological properties among different techniques.

From a purely mechanical perspective, braiding generally offers the highest tensile strength and fatigue resistance. Braided scaffolds are praised for their tubular design, excellent axial and radial load-bearing properties, and wear resistance,

Table 1 Mechanical properties of the native ACL and engineered scaffolds, categorized by fabrication methods and testing conditions (*in vitro vs. in vivo*)

	Polymer	Structure	Load at failure (N)	Stress at failure (MPa)	Strain at failure (%)	Stiffness (N mm^{-1})	Young's modulus (MPa)	Ref.
Native human ACL	Collagen	Hierarchical	2160 ± 157	—	—	242 ± 28	—	Woo *et al.*[78]
			2109	—	14.95	176	—	Elmarzougui *et al.*[79]
			1730 ± 0.66	37.8 ± 9.3	—	182 ± 56	—	Noyes *et al.*[80]
			Male: 1818 ± 699	—	—	Male: 308 ± 89	Male: 128 ± 5	Marieswaran
			Female: 1266 ± 527	—	—	Female: 198 ± 88	Female: 99 ± 50	*et al.*[81]
Initial mechanical properties tested before implantation								
Hamstring tendon	Collagen	Hierarchical	3790–4140	—	—	776	—	Rittmeister *et al.*[82]
Leeds-Keio	Polyester	Woven	Nonconditioned: 2061 ± 31	—	—	Nonconditioned: 151 ± 91	—	Matsumoto *et al.*[83]
			Preconditioned: 2350 ± 28			Preconditioned: 294 ± 26		
			2000	—	—	270	—	Legnani *et al.*[84]
LARS	PET	Knitted, twisted	1584–4720	—	8–10	89–321	—	Jedda *et al.*[85]
Synthetic materials	CANT	Woven	15 ± 1	∼40	104 ± 50	—	∼150	Laranjeira *et al.*[34]
	CANT	Braided	1.7	∼52	48 ± 12	—	∼450	
	Nylon 6,6	Electrospun	330 ± 11	22.9 ± 5	8.58 ± 0.2%	—	343 ± 87	Sensini *et al.*[86]
	PET	Leno woven	2181.36	—	45.54	119.75	—	Aka *et al.*[87]
	PET	Narrow woven	2968.52	—	43.13	172.07	—	
	PCL	Woven	272.6 ± 13.5	70 ± 3.5	75	—	1161.1 ± 9.3	Savić *et al.*[88]
	PGA, silk, PCL	2/2 Woven	—	46.37 ± 1.28	∼34	∼125	—	Xie *et al.*[66]
		4/2 Woven	—	48.58 ± 0.19	∼25.5	∼195	—	
	Polyamide	Braided	4161 ± 93.98	—	16.33 ± 1.04	219.97 ± 30	—	Jedda *et al.*[85]
	Polyester	Braided	3079 ± 168.69	—	15.44 ± 0.68	169.49 ± 15	—	
	UHMWPE	Knitted	1768.98 ± 62.65	—	34.68 ± 1.34	70.46 ± 9.2	—	
		Braided (10 cores)	5114.45 ± 339.37	502.46 ± 33.34	27.94	—	—	Huang *et al.*[49]
		Braided (14 cores)	5383.37 ± 568.42	415.83 ± 43.91	23.12	—	—	
		Braided (18 cores)	6499.60 ± 532.99	399.74 ± 32.78	7.73	—	—	
Biomechanical properties tested after 8/16/24 weeks of implantation								
Natural materials	Silk fibre, collagen matrix	Knitted, crosslinked	85.07 ± 8.3	—	—	10.42 ± 1.51	—	Bi *et al.*[63]
	Silk	Knitted	8 weeks: 45.48 ± 8.18	—	8 weeks: 13.4 ± 4.27	8 weeks: 3.58 ± 0.99	—	Fan *et al.*[53]
			16 weeks: 24.97 ± 5.21	—	16 weeks: 12.19 ± 3.89	16 weeks: 2.13 ± 0.49	—	
			24 weeks: 24.59 ± 1.64	—	24 weeks: 8.06 ± 3.16	24 weeks: 3.41 ± 1.21	—	
Synthetic materials	PCL	Electrospun	13.6 ± 2.4	—	—	7.1 ± 1.8	—	Leong *et al.*[89]
	UHMWPCL	Electrospun	24.6 ± 4.7	—	—	8.6 ± 2	—	Leong *et al.*[62]
	PGA. silk, PCL	Woven, electrospun	37.52 ± 7.15	—	30.04 ± 1.26	33.33 ± 4.65	—	Xie *et al.*[66]

Abbreviations: CANT – PCL/chitosan (CHT)/cellulose nanocrystals (CNC); leno weaving creates stable, open-mesh fabrics by twisting warp threads around each other; narrow weaving produces strong, small-width fabrics like ribbons and straps using specialised narrow looms; 2/2 Woven: 2 up and 2 down woven structures; 4/4 Woven: 4 up and 2 down woven structures.

Table 2 Comparative summary of scaffold and graft types based on the fabrication strategy, mechanical performance, degradability, and biological integration potential

Graft/scaffold type	Tensile strength (N)	Stiffness (N mm^{-1})	Key strengths	Key limitations	Ref.
Native human ACL	1730–2160	176–242	Anisotropic, viscoelastic, excellent fatigue life	N/A	Woo *et al.*,[78] Elmarzougui *et al.*,[79] Noyes *et al.*[80]
Autograft (hamstring tendon)	3790–4140	776	Excellent biocompatibility, no disease risk	Donor site morbidity, limited source, variable size/quality	Rittmeister *et al.*[82]
LARS ligament	1584–4720	89–321	High initial strength, immediate stability	Debris-induced synovitis, fatigue fracture, mechanical mismatch	Jedda *et al.*[85]
Leeds-Keio ligament	2000–2350	151–294	Good initial strength, biological inertness	Limited fatigue resistance, poor long-term tissue integration	Matsumoto *et al.*[83]
Weaving	2181–2968	119–195	High anisotropy, customisable properties, no delamination	Complex fabrication, potentially lower fatigue resistance than braiding	Aka *et al.*,[87] Xie *et al.*[66]
Braiding	3079–6499	169–219.97	Highest tensile strength and fatigue resistance	Isotropic properties, limited porosity control, less anatomical shape	Jedda *et al.*,[85] Huang *et al.*[49]
Knitting	1768.98 ± 62.62	70.46 ± 9.2	High flexibility and conformity, large pores	Low strength and stiffness, prone to unravelling, high creep	Jedda *et al.*[85]
Electrospinning	330 ± 11	—	Excellent ECM mimicry, high surface area	Very poor mechanical properties, small pores, difficult to handle	Sensini *et al.*[86]

making them ideal for tissue augmentation. This is due to the narrow yarn interweaving angles, which more closely align the fibres with the load-bearing axis. However, their limited porosity can inhibit tissue ingrowth,[74] while the locking angle during braiding can increase stiffness and impair stress–strain behaviour, potentially leading to plastic deformation.[74]

Knitted structures are more porous and less stiff, resulting in the most compliant scaffolds. Their large open-loop allows for enhanced cellular infiltration and greater internal connectivity, supporting connective tissue formation.[90] Despite these positive cellular responses, knitted structures generally lack the ultimate strength, strain and fatigue resistance of native ligaments, making them mechanically unsuitable for load-bearing ACL replacement.

Electrospinning is a versatile technique capable of producing nanofibrous scaffolds that mimic the extracellular matrix (ECM), providing a highly porous environment conducive to cell adhesion, proliferation and differentiation.[91] However, electrospun scaffolds exhibit poor mechanical strength and stability under physiological loads, and their dense pore structure sometimes can hinder cellular infiltration.[92] They are not effective as standalone ACL grafts.

Weaving technology, in contrast, stands out for its unique ability to replicate the hierarchical structure of human tissues.[93–95] The weaving process enables the creation of multilayered, fibre-oriented structures that closely mimic the natural alignment of collagen fibres. The key advantages of woven structures lie in their tunability and anisotropy. By carefully controlling the weave pattern, it is possible to produce fibre bundles aligned in a manner similar to the native tissue's collagen orientation.[96–101] By using stronger yarns in the warp direction and more compliant yarns in the weft, woven scaffolds can be designed to be stiff along their length while allowing for some flexibility in the transverse direction, better mimicking native tissue.[102]

However, even for scaffolds made of similar materials or fabrication methods, the mechanical properties reported in Table 1 vary significantly across studies. This variability can be attributed to differences in experimental protocols, such as sample geometry, testing speed, hydration conditions *etc.* *In vivo* studies further introduce biological variability due to differences in animal models, healing duration and biological remodelling processes. Additionally, some studies report mechanical properties testing immediately after fabrication, while others assess the scaffolds weeks or months after implantation, making direct comparisons challenging. Therefore, while the values in the table provide a useful benchmark, interpretation of scaffold performance still requires consideration of these specific factors.

5. Structural design and fabrication of woven scaffolds

Weaving technology offers flexibility in designing scaffolds that biomimic the complex structure of the natural ACL. As a

mature and highly controllable manufacturing process, weaving technology enables the rational design of grafts with customised properties. The biomechanical and biological performance of woven scaffolds depends on the interplay between material selection, yarn characteristics (*e.g.*, linear density and filament count), and, most importantly, the weave architecture. Advanced weaving techniques enable the fabrication of structures with regional characteristics, controlled porosity and anisotropic mechanics, far exceeding those of simple fabric structures.

5.1. Overview of weaving techniques

Weaving, one of the earliest textile techniques documented for making fabrics,[103] is a complex process involving the interlacing of longitudinal warp yarns parallel to the fabric's length, with transverse weft yarns passing through the warp yarns to create a woven fabric. This weaving procedure can be accomplished manually using a hand loom or mechanically by a power loom, which is the case for the modern textile industry. The process, after the warp preparation, typically involves several sequential steps, including shedding, weft insertion, beat-up, take-up, and let-off, as detailed in Fig. 2, resulting in a woven structure with a specific pattern.[104] By altering the shedding motion, a variety of weave patterns can be achieved.

5.2. From 2D layers to integrated 3D structures

The basic weaving forms for biomedical applications are flat and tubular weaving. Early attempts at woven ACL scaffolds utilised these traditional two-dimensional (2D) techniques, which produce flat fabrics that can be rolled or layered to form a ligament-like structure. The most common weave patterns are plain, twill and satin weaves, respectively, as shown in Fig. 3. In the plain weave, each weft yarn alternates over and under each warp yarn, forming a dense structure with maximum binding points and minimal floats, which enhances stability but reduces elasticity, and relatively low porosity. The twill weave is characterised by a diagonal pattern on the fabric surface as each weft yarn crosses over and under multiple warp yarns, with a ''step'' or offset between rows. This results in a more pliable, porous and flexible fabric than a plain weave, better suited to conforming to the human anatomy. The satin weave differs by allowing a warp yarn to float over four or more weft yarns before passing under one, resulting in fewer binding points and longer floats compared to plain and twill weaves. This weave provides a very smooth surface and high drapability. However, the long, unsupported yarn segments are easily snagged and may exhibit lower structural integrity under abrasive conditions within the joint. Although twill and satin fabrics have lower structural stability, they offer greater elasticity and higher tear strength due to the yarn movement and aggregation,[108,109] which mimics the resistance to breakage of human soft tissues.[110] Additionally, satin fabrics exhibit asymmetry, with warp yarns mainly on the satin side and weft yarns on the opposite side, providing unique properties when the warp and weft yarns have different cellular affinities or mechanical characteristics.[111]

These 2D woven structures have been used as scaffolds in tendon, ligament and bone tissue engineering. For example, Savić *et al.*[88] developed a PCL fabric by first producing continuous electrospun filaments, which were then stretched, twisted into yarns, and woven as shown in Fig. 4. This woven electrospun (ES) fabric achieved a strength of 272.6 N, exhibiting greater compliance (lower Young's modulus) (116 MPa *vs.* 1441 MPa) and higher strain-to-failure (75% *vs.* 36%) than clinical FiberWire sutures. Biologically, the fabric was non-cytotoxic and supported a three-fold increase in human ACL-derived cell proliferation over two weeks, promoting elongation and alignment cell morphology.

Another innovative approach involves combining different fibre scales. Cai *et al.*[72] used electrospun nanofiber yarns (PLLA or silk fibroin (SF)/PLLA) as the weft and commercial PLLA microfiber yarns as the warp creating the nmPLLA and nmSF/PLLA scaffolds dispatched in Fig. 5. These hybrid scaffolds exhibited significant anisotropy, with enhanced strength and stiffness in the weft direction due to the higher weave density of the nanofiber yarns. After six months of *in vivo* experiment, the nmSF/PLLA scaffold demonstrated biomechanical properties comparable to the native Achilles tendon and significantly promoted tenocyte adhesion, proliferation and immunomodulatory functions.

While these 2D fabrics can be layered to create 3D grafts, this approach has a critical drawback: the potential for interlaminar delamination. Under the complex shear and torsional forces experienced in the knee joint, these layers can separate, leading to graft failure.[112] This fundamental limitation has driven the field towards true 3D weaving techniques.

5.3. Advanced 3D weaving for anatomical biomimicry

The transition from simple 2D fabrics to integrated 3D structures represents a paradigm shift in designing scaffolds capable of replicating the ACL's complex anatomy. 3D weaving technologies were initially developed for the aerospace and composite industries, where they are used as reinforcement materials. The reinforcements are combined with selected matrices to form fibre-reinforced polymer (FRP) materials, which enhance mechanical properties through the thickness for use in ballistic, aerospace, automotive and structural reinforcement applications.[113–115] The growing interest in utilising textile products in a variety of applications has nowadays driven the idea of developing 3D fabrics into tissue engineering. In contrast to the 2D fabrics, 3D weaving technology offers the possibility of producing custom-designed 3D structures for use as scaffolds in cell growth, offering a more suitable environment that closely mimics the natural cell growth and development, thus allowing the replacement of different types of tissues.[116] In contrast to 2D fabrics, where yarns are interwoven only in the *X*–*Y* plane, 3D fabrics allow yarns to interlace both in the *X*–*Y* plane and along the *Z*-axis, which is perpendicular to the plane, mechanically locking the layers together. This integral construction eliminates the risk of delamination, providing superior durability, enhanced structural stability, and the ability to create complex shapes.[113]

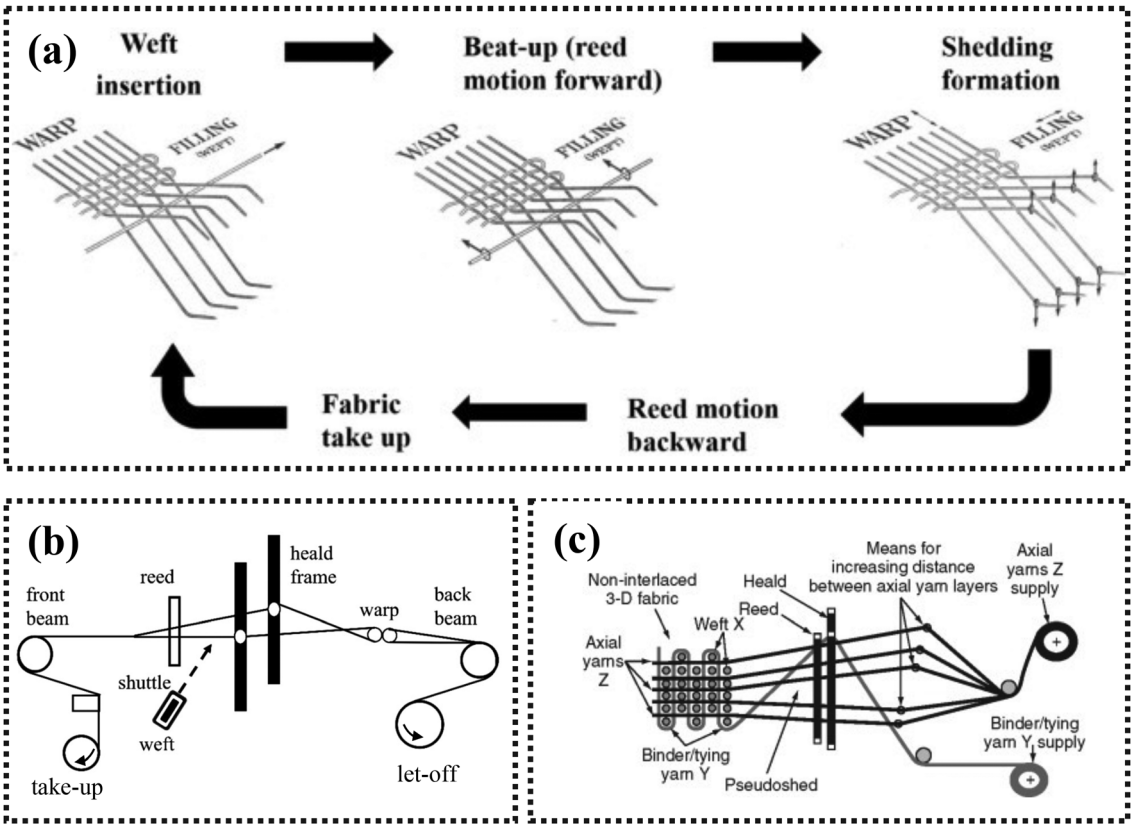

Fig. 2 Weaving processes. (a) A complete loom motion.[105] Reproduced with permission, copyright 2019, Elsevier. (b) 2D weaving process.[106] Reproduced with permission, copyright 2023, Sage Publications. (c) 3D weaving process.[107] Reproduced with permission, copyright 2008, Elsevier.

3D woven fabrics are categorised into several types, including solid, hollow, shell, and nodal structures,[117] which refer to dense, lightweight, curved and interconnected designs, each tailored for specific functional applications. The most widely used 3D woven fabrics are solid structures[117] which include the orthogonal, angle-interlock and multilayer as shown in Fig. 6. The orthogonal structure is characterised by three sets of interweaving yarns that are perpendicular to each other, known as *X*, *Y* and *Z* yarns, as depicted in Fig. 6(a). The key function of *Z* yarns is to interconnect the individual warp and weft yarns to solidify the fabric's structure. The angle interlocking structure consist of layers of straight weft yarns and a set of crimped warp yarns, as shown in Fig. 6(b), that weave with the weft yarns diagonally through the thickness. If needed, the wadding warp yarns can be introduced into the fabric to offer more balanced mechanical behaviour between the *X* and *Y* directions of the fabric. Multilayer structure typically features multiple fabric layers, each with its own warp and weft yarns, as shown in Fig. 6(c). These different layers are connected by self-stitching using existing yarns or by central stitching using external yarns. The application of

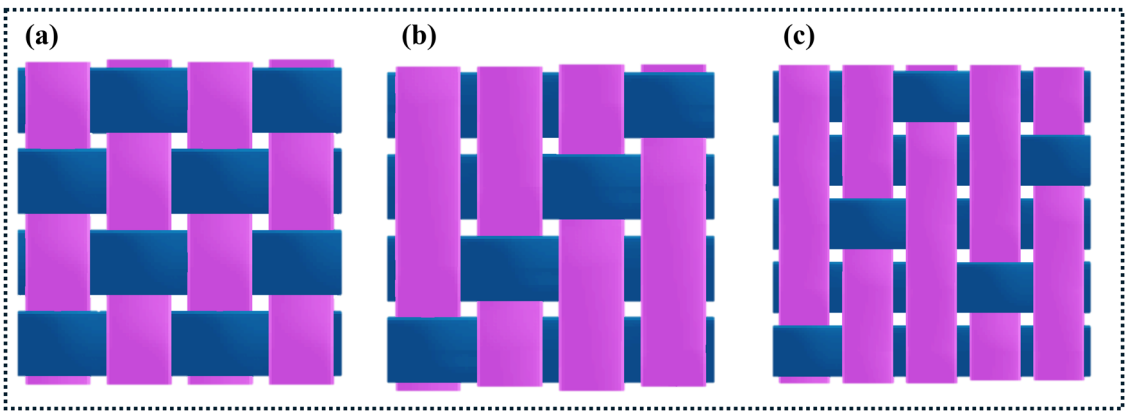

Fig. 3 Schematic of 2D woven patterns: (a) plain, (b) twill and (c) satin.

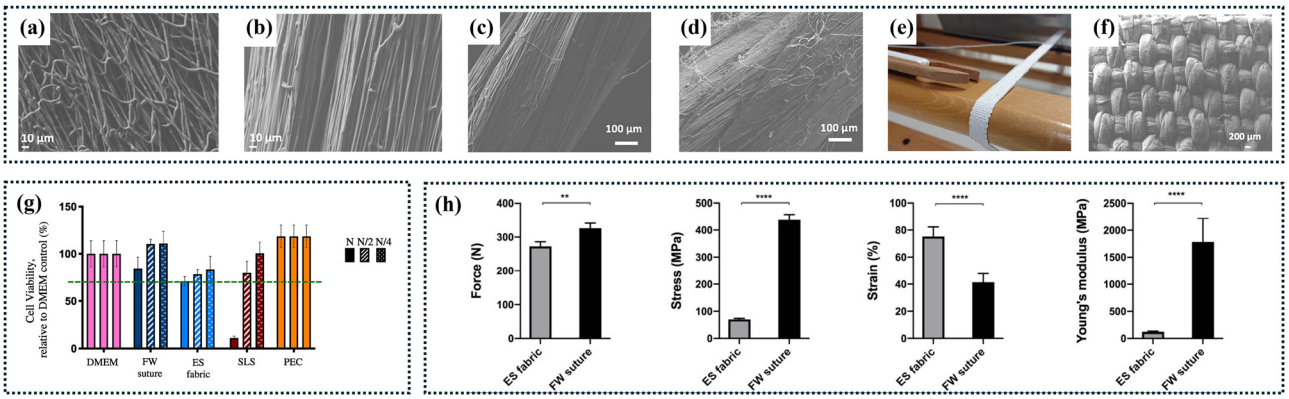

Fig. 4 Producing stretched filament and woven into the fabric for ACL reconstruction.[88] Reproduced with permission, copyright 2021, Elsevier. (a) SEM image of collected, unstretched filaments with the random microfibre arrangement. (b) SEM image of stretched filaments with the aligned microfibre arrangement. (c) SEM image of a plied yarn. (d) SEM image of a cabled yarn. (e) and (f) A handloom was used to produce a band with a plain weave structure. (g) Cytotoxicity of the ES fabric compared to the FW suture. *N* represents the undiluted extract. *N*/2 and *N*/4 represent 2-fold and 4-fold dilutions of *N*, respectively. DMEM represents the medium only (vehicle) control group; SLS (sodium dodecyl sulphate) represents the positive control group; PEC (polyethylene caps) represents the negative control group. (h) Mechanical properties (maximum force, maximum stress, strain at maximum stress and Young's modulus) of the ES fabric compared to FW sutures (control).

these structures to ACL reconstruction allows creating a single, integrated graft with functionally distinct regions that mirror the native ligament's path from the intra-articular region into the bone tunnels. Several key strategies have emerged:

Hierarchical core-sheath designs: The native ACL is composed of axially aligned collagen fibres organised into a hierarchical structure with multiple levels of aggregation, all encased within a collagen fibre membrane. To mimic this hierarchical structure, Aka *et al.*[87] developed a core-sheath structure using conventional weaving techniques. They used straight parallel yarns as the core to bear the primary axial load, while a narrow-woven or a leno-woven outer sheath provided containment and stability. Results showed that the

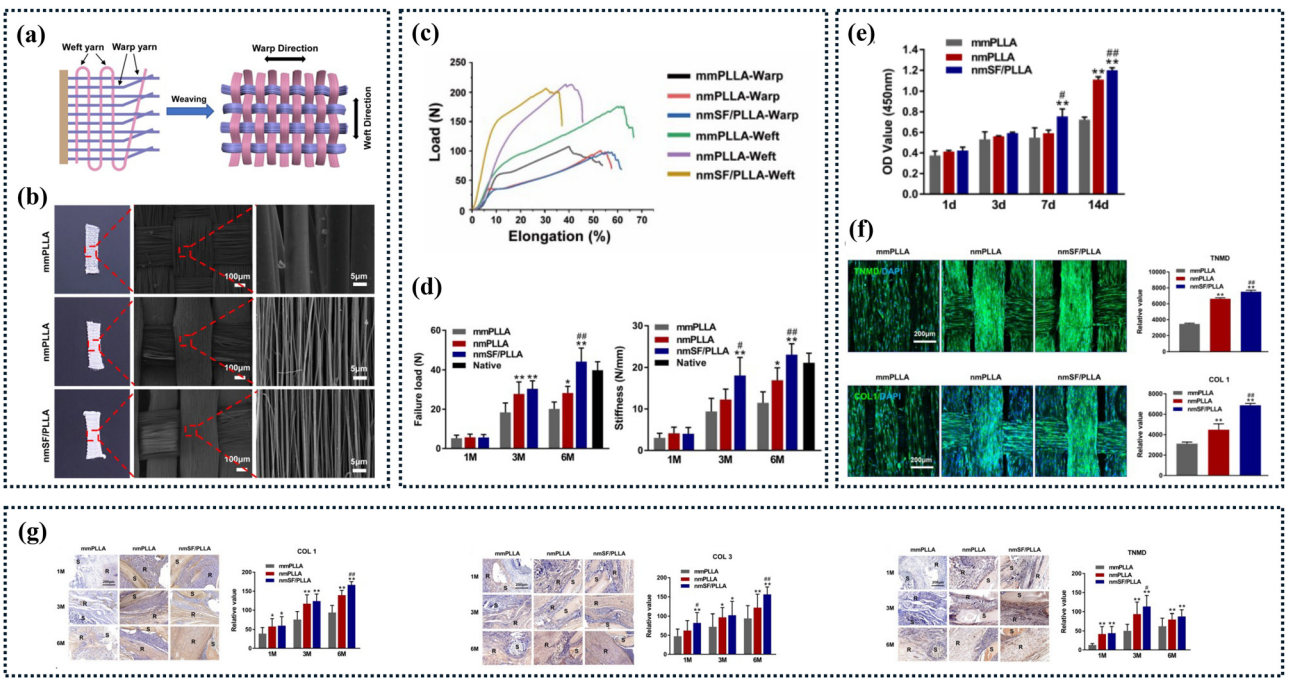

Fig. 5 Nano-micro 2D fibrous woven scaffolds in tendon engineering.[72] Reproduced with permission, copyright 2023, IOPscience. (a) and (b) Fabrication and morphology of mmPLLA, nmPLLA and nmSF/PLLA scaffolds. (c) Load–elongation curves of mmPLLA, nmPLLA and nmSF/PLLA scaffolds along warp and weft directions. (d) Biomechanical properties (failure load and stiffness) at 1, 3 and 6 months after surgery in the three groups and native mouse Achilles tendon. (e) Tenocyte proliferation on the three scaffolds after 1, 3, 7 and 14 days of culture. (f) TNMD and COL1 proteins for tenocytes on the three scaffolds after 14 days of culture. (g) Immunohistochemistry staining and semi-quantitative analysis of collagen type 1 (COL1), collagen type III (COL3) and tenomodulin (TNMD) for regenerative tissues at 1, 3 and 6 months after surgery in the three groups. $*P < 0.05$; $**P < 0$; $\#P < 0.05$ compared with the nmPLLA group; $\#\#P < 0.01$ compared with the nmPLLA group. S, scaffold; R, regenerated tissue.

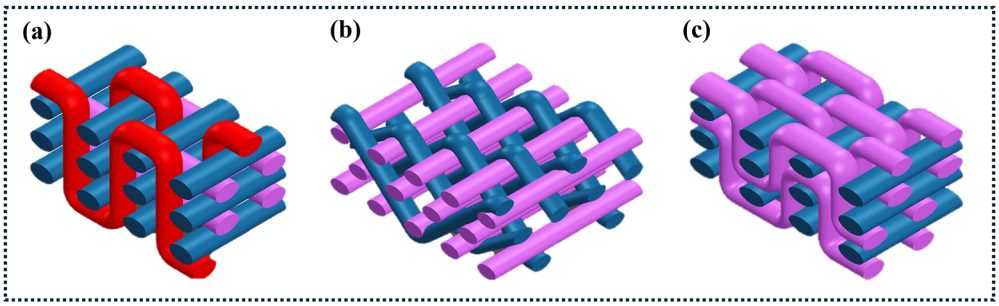

Fig. 6 3D solid woven fabrics: (a) orthogonal, (b) angle interlock and (c) multilayer.

narrow-woven ligament effectively replicated the fascicle-like architecture of the native ligament.

Functionally graded hybrid structures: The ligament-to-bone insertion is a complex gradient interface. To replicate this, Xie *et al.*[66] combined weaving and electrospinning technologies to design a multilayered scaffold as shown in Fig. 7. The woven core utilizes a gradient degradation design, using fast-degrading PGA and slower-degrading silk yarns to form

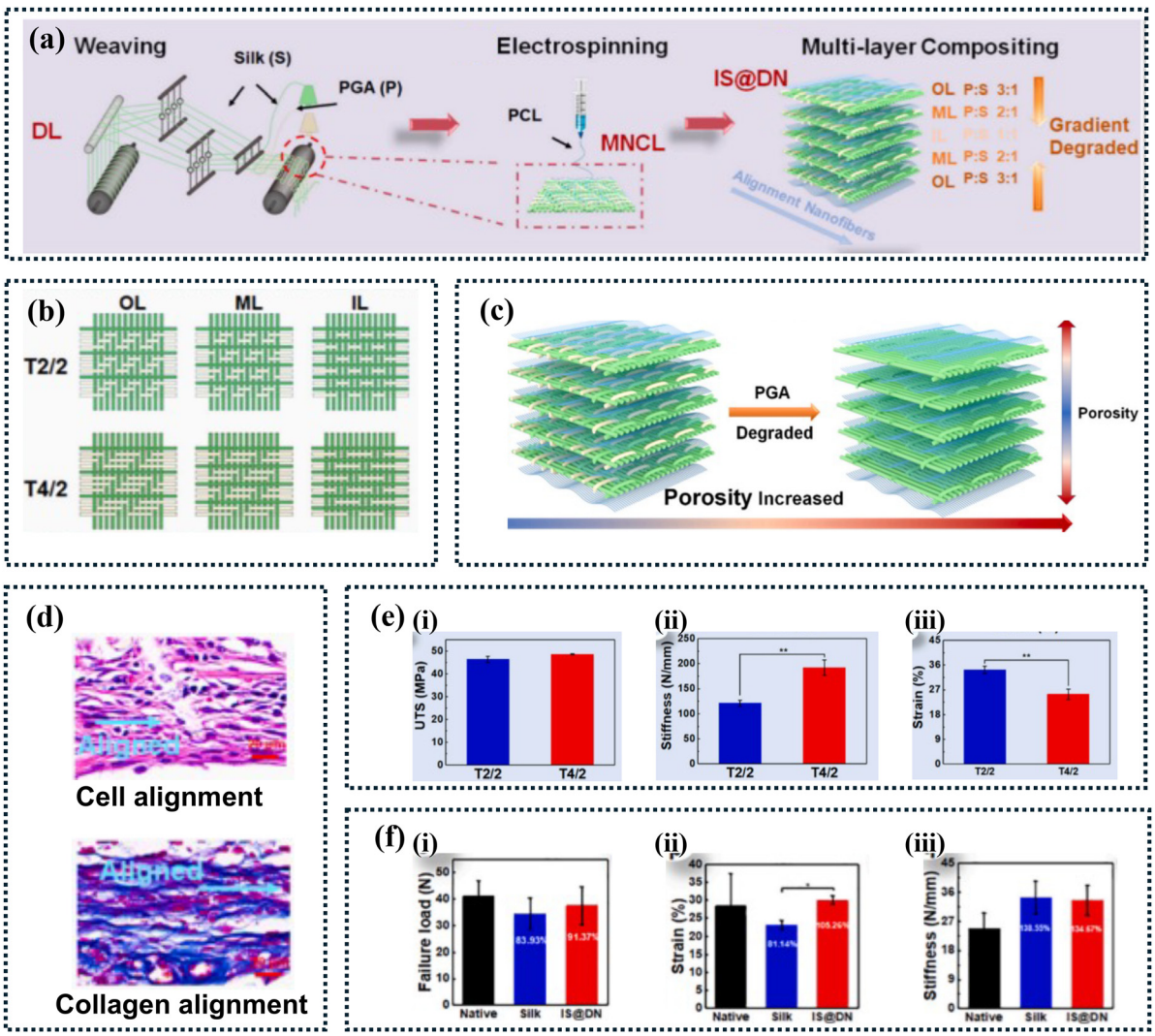

Fig. 7 Multilayer woven scaffolds for tendon reconstruction.[66] Reproduced with permission, copyright 2024, Elsevier. (a) Fabrication of the multilayer composite (IS@DN), showing the degraded layer (DL) and micro-nanocomposite layers (MNCLs). (b) Structural schematics of T2/2 and T4/2 scaffolds, delineating outer (OL), middle (ML), and inner (IL) layers. (c) Illustration of IS@DN's gradient degradation. (d) Cell and collagen alignment observed at 4 weeks. (e) Mechanical characteristics of IS@DN: (i) ultimate tensile stress, (ii) stiffness, and (iii) strain. (f) Biomechanical performance of regenerated Achilles tendons at 8 weeks: (i) failure load, (ii) strain, and (iii) stiffness. T2/2: right twills with wefts 2 up and 2 down; T4/2: right twills with wefts 4 up and 2 down.

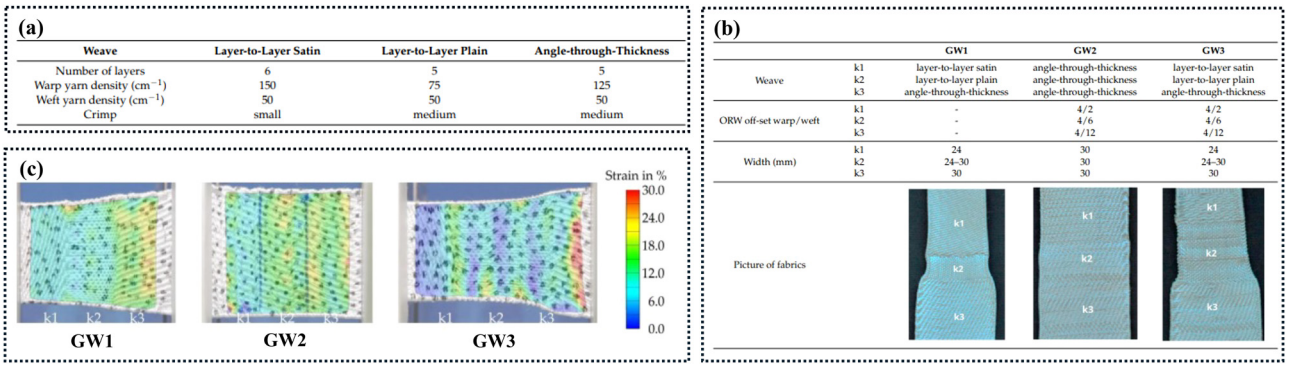

Fig. 8 Multilayer woven fabrics with different number of layers, warp density and crimps used for the artificial ligament.[118] Reproduced under the terms and conditions of the Creative Commons Attribution (CC BY) license. (a) Parameters of layer-to-layer satin, layer-to-layer plain and angle-through-thickness woven fabrics. (b) 3D gradient woven structures. (c) The strain in the individual zones of the gradient weave structures.

channels for cell infiltration over time. This was then composited with electrospun PCL nanofibers to provide a nanoscale topographical structure to guide cell alignment. This hybrid approach created a functionally graded implant that successfully promoted both tissue infiltration and organized tissue formation in a rat model.

Anatomically shaped 3D woven scaffolds: The most advanced approach uses true 3D weaving to create scaffolds with both gradient properties and anatomical shapes directly on the loom. This "near-net-shape" manufacturing process has significant advantages. Lang *et al.*[118] demonstrated the ability to create gradient properties by weaving a single fabric with three distinct regions, layer-to-layer satin, angle-through-thickness, and layer-to-layer plain weaves. This allowed them to precisely control the crimp at different sections of the implant, thereby controlling stiffness and elongation. However, a crucial limitation of this work is the lack of biological properties verified through either *in vitro* or *in vivo* experiments.

Collectively, these studies highlight the significant potential of 3D weaving technologies in tissue engineering. 3D weaving technology goes beyond conventional textile structures, enabling the fabrication of integrated, multi-zonal and anatomical structures that closely replicate the hierarchical structure and biomechanical function of the native ACL. While promising results have been reported in small animal models, the lack of studies in large animal models remains a key barrier to clinical translation. Finite element analysis (FEA) has been applied to simulate the complex mechanical behaviour of ligament scaffolds under tensile loading (Fig. 8). However, its integration into the practical design and validation of ACL grafts remains limited. Future studies could focus on combining large animal *in vivo* studies with predictive computational models, alongside comprehensive evaluation of cell–scaffold interactions, including ECM deposition and tissue remodelling to better guide scaffold design and accelerate clinical advancement.

5.4. The structure and function relationship

The advantage of weaving is its ability to establish predictable links between structural parameters and functional outcomes, enabling a rational and adaptable approach to ACL scaffold design. As illustrated in Fig. 9, key textile parameters like yarn type, weave density and fibre alignment determine scaffold properties including the mechanical strength, porosity, pore size and degradation rate. These material-level properties directly influence biological responses such as cell adhesion, alignment, tissue integration and immune modulation, highlighting the importance of an integrated understanding of structure and function during scaffold development.

5.4.1. Weave pattern, yarn density and anisotropy. The choice of weave pattern and the density of warp and weft yarns are the primary tools for controlling mechanical anisotropy. For the ACL, high stiffness and strength are desired in the longitudinal axis, while greater compliance is needed in the transverse direction. As demonstrated by Gilmore *et al.*[119], fundamental process parameters including fibre geometry, fabric structure and material composition are essential for effective weaving because they significantly influence the scaffold permeability, thereby affecting various aspects of tissue healing from initial ECM formation to subsequent calcification. This inherent adaptability gives woven structures significant advantages over other textile forms. By using high-modulus, high-density warp yarns and more flexible, lower density weft yarns, woven scaffolds can effectively mimic this anisotropic behaviour.[120] The study by Lang *et al.*[118] previously discussed in Section 5.2 shows a clear correlation where different weave patterns altered yarn crimp, allowing for precise control of the elongation and stiffness of distinct scaffold regions. Moreover, Aka *et al.*[87] directly compared the leno woven PET scaffold with the narrow woven one. The narrow woven structure, which generally has a higher yarn density and more stable interlacing, exhibited significantly higher ultimate tensile strength (2968 N *vs.* 2181 N) and stiffness (172 N mm^{-1} *vs.* 120 N mm^{-1}) compared to the more open leno weave. Similarly, Xie *et al.*[66] investigated the effect of twill weave patterns on hybrid PGA/silk/PCL scaffolds. They found that changing the 2/2 twill to a 4/2 twill (a change that affects yarn crimp and float length) increased the tensile stress from 46.4 MPa to 48.6 MPa and substantially improved the stiffness from approximately 125 N mm^{-1} to 195 N mm^{-1}. These studies provide concrete quantitative evidence that weaving parameters are not just

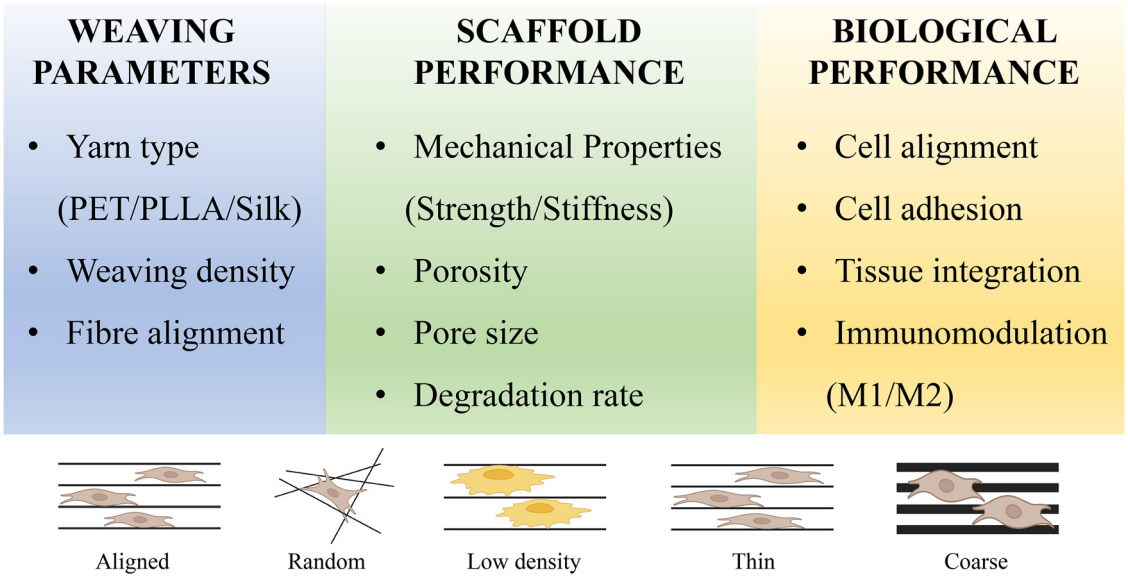

Fig. 9 Schematic illustrating how weaving parameters influence scaffold properties and biological responses. Input parameters (*e.g.*, yarn type, weave density, and pore size) determine the mechanical and structural properties, which in turn affect cell adhesion, alignment, tissue integration, and immune modulation.

design inputs but are direct levers for achieving engineered, predictable functional outcomes, allowing for precise tuning of woven scaffolds to meet the demanding biomechanical environment of the knee.

5.4.2. Engineering the micro-environment for biological response. In addition to overall mechanical properties, weaving allows for the precise engineering of the scaffold's microenvironment, which is critical for guiding cellular behaviour and promoting tissue integration. Almost all tissue cells grow within the ECM featured by the complex 3D fibrous network, and this has been supported by previous studies illustrating that 3D substrates exhibit higher bioactivity and increased rates

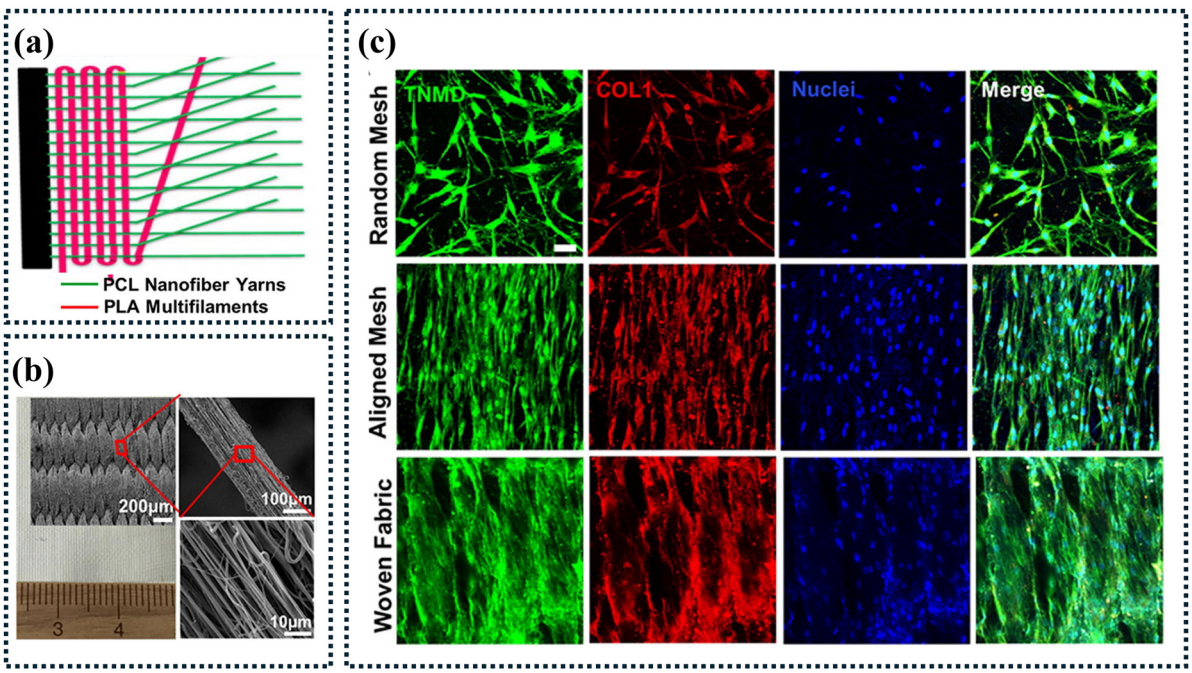

Fig. 10 Woven nanofibrous scaffolds promote tendon-related gene expression in human tenocytes.[102] Reproduced with permission, copyright 2017, Elsevier. (a) Schematic showing the textile weaving process. (b) SEM image of the plain weave fabric made of PCL nanofibre yarns with a high density (100 picks per cm) as weft and PLA multifilaments with a lower density (55 ends per cm) as the warp. (c) Woven fabrics improved the expression of tendon-associated gene markers in human tenocytes (HT) compared to the random and aligned meshes. Immunofluorescence staining for TNMD (green), COL1 (red), and nuclei (blue).

of cellular migration and proliferation surpass that of the 2D substrates.[121–124] The advantages of 3D matrices are their ability to create cellular supports with diverse physical appearances, porosity, mechanical properties and nanoscale surface features, thus enabling each cell type to thrive in a distinct 3D microenvironment.[125,126] Key parameters include pore size, Fibre diameter and porosity.

5.4.2.1. Pore size. The pore size of scaffolds is a key factor influencing cell behaviour, including adhesion, proliferation, migration and differentiation. A delicate balance is required.[127] Smaller pores provide a greater surface area for initial cell attachment,[128] but can impose spatial constraints that limit cell migration and lead to surface-only colonization. Conversely, larger pores improve cell migration, nutrient diffusion, and 3D cellular organisation, but can compromise initial cell adhesion if too large. Wu *et al.*[102] demonstrated that 2D woven fabrics with large, controllable pore sizes (12.2 ± 1.1 μm) better supported cell proliferation and infiltration compared to electrospun meshes with much smaller pores by co-culturing or tri-culturing these woven fabrics with large pores, along with human adipose-derived mesenchymal stem cells (hASC), human tenocytes (HT), and/or human umbilical vein endothelial cells (HUVEC) under dynamic mechanical conditions (Fig. 10). The optimal pore size is highly cell-type-dependent, with studies showing that osteoblasts proliferate best in pores of 96–190 μm, while fibroblasts thrive in the 40–80 μm range.[129–134]

5.4.2.2. Fibre diameter. Fibre diameter influences cell adhesion, spreading, alignment, and differentiation. Smaller fibre diameters, typically in the nanometre range, increase the surface area for cell attachment, promoting enhanced cell adhesion and encouraging cells to spread and elongate.[135] Conversely, larger fibre diameters provide more structural stability, supporting cell proliferation and offering more surface area for cell attachment.[136] The scaffold stiffness, influenced by fibre diameter, can further affect the differentiation of cells, which respond to changes in substrate rigidity.[137] Thus, the fibre diameter of scaffolds must be carefully optimised to suit the specific needs of the target cell type and tissue application, balancing factors like mechanical support, cell alignment and differentiation potential.

5.4.2.3. Porosity. High porosity enhances cell migration and infiltration into the scaffold and improves the delivery of nutrients, oxygen and waste removal.[138] In addition, porosity facilitates the formation of 3D cellular networks, enabling more natural cell–cell interactions and promoting the development of tissue-like structures.[139] However, excessive porosity weakens the scaffold's mechanical strength and stability, which can affect cells that are sensitive to mechanical cues.[137,139] Therefore, achieving a balance between porosity and mechanical integrity is critical.

5.5. Hybrid yarns and multi-component structures

Advanced ACL scaffolds increasingly rely on hybrid strategies that integrate multiple approaches to achieve multiscale, multifunctional performance. These strategies combine complementary

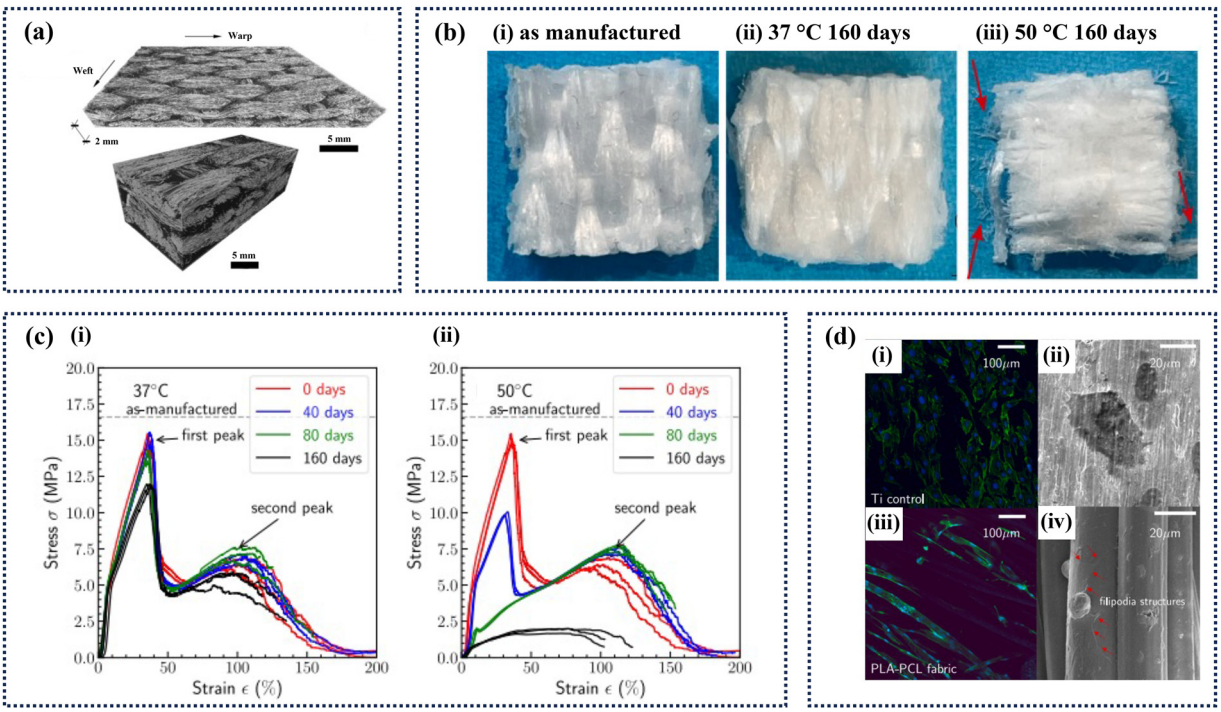

Fig. 11 Characterisation of PLA/PCL fabrics and cellular interaction.[141] Reproduced under the terms of the Creative Commons CC-BY license. (a) X-ray tomograms of the PLA/PCL fabric. (b) PLA/PCL woven fabrics (i) as manufactured (0% mass loss); (ii) 160-day PBS immersion at 37 °C (1% mass loss); (iii) 160-day PBS immersion at 50 °C (17% mass loss). The red arrows denote debris. (c) Stress–strain curves of PLA/PCL fabrics after PBS immersion at (i) 37 °C and (ii) 50 °C. (d) Confocal microscopy and SEM images of MC3T3-E1 pre-osteoblast interaction with sample surfaces (24 hours post-seeding). (i) and (ii) Ti control; (iii) and (iv) PLA/PCL textile. The red arrows in (iv) indicate filipodia structures (cell–material interaction).

strengths in fabrication techniques, material properties and surface chemistry to overcome individual limitations. An example is the integration of weaving with electrospinning. Xie *et al.*[66] demonstrated how a woven core can provide macroscale mechanical strength, while an electrospun nanofiber layer introduces nanoscale topology that promotes cell alignment, effectively combining structural integrity with biological guidance. Similarly, Rashid *et al.*[140] and Savić *et al.*[88] showed that composite structures with a woven mechanical layer and an electrospun bioactive interface could enhance fibroblast infiltration and neovascularisation *in vivo*. At the material level, Pereira-Lobato *et al.*[141] developed commingled PLA/PCL yarns that combine the stiffness of PLA with the ductility of PCL to produce a textile with a favourable balance of strength and resilience (Fig. 11). Surface functionalisation also plays a key role in hybrid design; for instance, Cai *et al.*[72] applied a calcium-phosphate coating to PET scaffolds *via* electrochemical deposition, significantly improving osteoblast adhesion and osseointegration at the bone–ligament interface. Although such strategies are already being explored in ACL scaffold development, current applications remain relatively limited. Further research is needed to systematise and expand these approaches, ultimately enabling the design of clinically viable scaffolds that meet both mechanical and biological demands.

6. Challenges and future directions

While woven scaffolds hold great promise, translating them from laboratory prototypes to standard clinical treatments remains a complex and multifaceted challenge. The future of the field will depend on addressing key translational barriers, employing patient-specific design strategies and integrating emerging technologies to develop truly functional, next-generation ligament implants.

6.1. Clinical translation and long-term performance

A major challenge in the field is bridging the translational gap between promising preclinical outcomes and broad clinical applications. This gap is primarily due to the lack of long-term human trial data for advanced biodegradable woven scaffolds. Meeting the strict regulatory requirements of bodies like the FDA and EMA demands a level of data robustness that typically exceeds academic research standards. This includes comprehensive biocompatibility testing (ISO 10993), good manufacturing practice (GMP) – compliant scalable manufacturing, and extensive mechanical fatigue testing to ensure long-term reliability.

Moreover, most preclinical animal studies are limited to follow-up periods of one year or less, which is inadequate for evaluating final-stage scaffold degradation, last-stage tissue remodelling or potential delayed complications. Establishing multi-year studies in large animal models is therefore a critical and necessary step to confirm the durability and safety of any new scaffold design before human trials can be justified.

6.2. Patient-specific design and computational modelling

The future of ACL reconstruction is shifting away from a ''one-size-fits-all'' approach towards personalised treatment strategies. Among the available fabrication methods, weaving stands out for its tunability and design flexibility. A patient-specific scaffold could be customised based on anatomical differences captured by MRI, as well as factors such as age, gender and anticipated activity levels. For example, a professional athlete may benefit from graft engineering for high strength and fatigue resistance, whereas an older or less active patient might

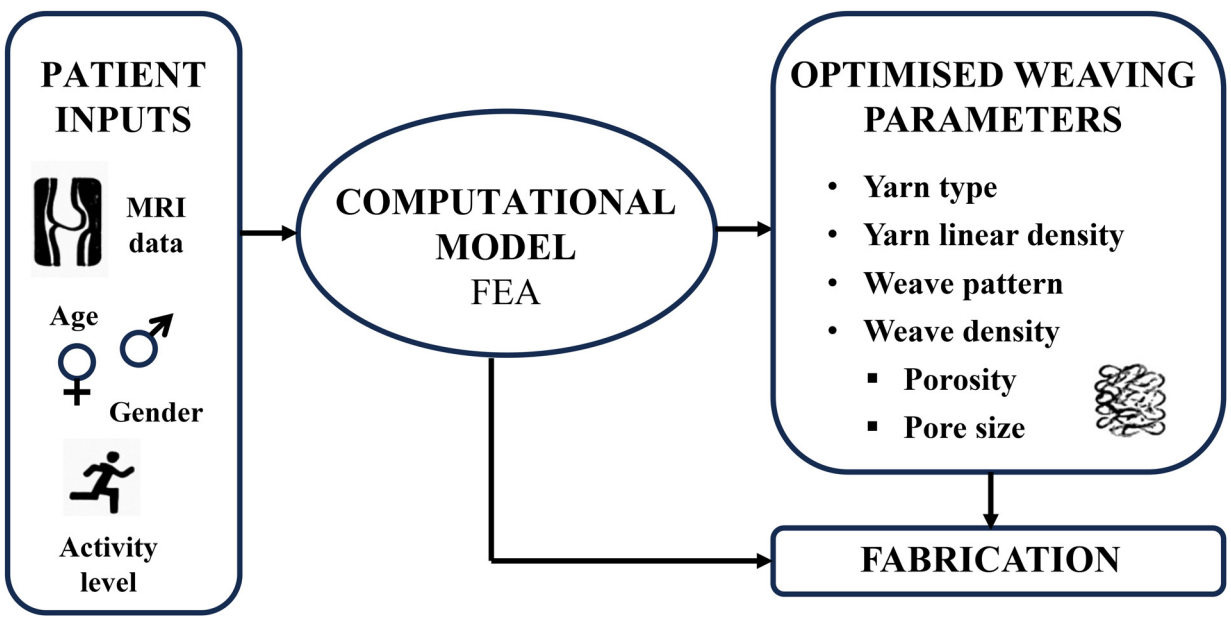

Fig. 12 Design workflow for patient-specific woven ACL scaffolds. Patient inputs (*e.g.*, MRI, age, sex, and activity levels) inform FEA, which guides the optimization of weaving parameters for personalized scaffold fabrication.

require a more compliant scaffold that promotes faster biological integration. FEA plays a critical role in this personalised design process. By simulating joint mechanics under physiological loading conditions, FEA allows engineers to optimise weave parameters including yarn type, yarn linear density, pattern and weave density to match the scaffold's mechanical performance with the patient's unique biomechanical profile (Fig. 12).

6.3. Emerging trends and hybrid strategies

The next generation of woven scaffolds will likely be ''smart'' textiles, incorporating mechanoresponsive materials or embedding biosensors to monitor the healing process. In addition, hybrid strategies that combine the architectural strength of weaving with complementary technologies to enhance overall performance are also promising. Examples include surface functionalisation techniques to improve material–cell interactions or integration of weaving with other fabrication methods such as electrospinning to create multiscale structures.[66,67,88,141] As these multi-component systems increase in complexity, artificial intelligence (AI) is expected to play a role by analysing large datasets from simulations and experiments, enabling more efficient prediction and optimization of scaffold designs compared to traditional research methods.

7. Conclusions and future perspectives

The reconstruction of the ruptured ACL remains a significant clinical challenge, with high re-rupture rates and a substantial incidence of post-operative osteoarthritis. Current grafts provide adequate mechanical strength but fail to replicate the native ACL's hierarchical structure and layered morphology, resulting in inflammation and poor tissue integration. Among textile fabrication techniques, weaving, particularly 3D weaving, stands out by enabling scaffolds with customisable mechanical properties and biomimetic architectures.

The ideal scaffold should replicate the native ACL's ultimate tensile strength (approx. 2000 N) and stiffness (approx. 240 N mm^{-1}) while providing a porous microenvironment (pore sizes of 40–190 μm) for cellular integration. While braiding offers high strength but limited structural complexity, knitting provides excellent porosity at the expense of mechanical performance, and electrospinning delivers nanoscale biomimicry but lacks sufficient durability. Weaving uniquely balances these requirements, achieving targeted mechanical properties, controlled porosity, and complex structures that mimic the ligament-to-bone transition.

Despite these advances, challenges remain in efficiently utilising fibre properties, ensuring secure scaffold fixation to bone and guaranteeing the long-term durability of biodegradable designs. Addressing these barriers will require continued innovation in textile engineering, advanced computational modelling and rigorous clinical trials. Future research should focus on integrating these approaches to translate the promise of woven scaffolds into reliable, durable, and biologically integrated solutions for ACL reconstruction.

Author contributions

Conceptualization, investigation, and writing – original draft: D. Y., F. S., and X. C.; funding acquisition: D.Y. and X. C.; writing – review and editing and supervision: X. C.

Conflicts of interest

The authors declare no conflicts of interest.

Data availability

No primary research results, software or code have been included and no new data were generated or analysed as part of this review.

Acknowledgements

The author Danjie Yang is financially supported by the China Scholarship Council [grant No. 202108420005].

References

1 J. J. Greiner, E. M. Nazzal, R. P. Reddy and J. D. Hughes, *Knee Arthroscopy and Knee Preservation Surgery*, Springer, 2023, pp. 1–15.
2 C. C. Kaeding, B. Léger-St-Jean and R. A. Magnussen, *Clin. Sports Med.*, 2017, **36**, 1–8.
3 D. J. Beard, L. Davies, J. A. Cook, J. Stokes, J. Leal, H. Fletcher, S. Abram, K. Chegwin, A. Greshon, W. Jackson, N. Bottomley, M. Dodd, H. Bourke, B. A. Shirkey, A. Paez, S. E. Lamb, K. Barker, M. Phillips, M. Brown, V. Lythe, B. Mirza, A. Carr, P. Monk, C. Morgado Areia, S. O'Leary, F. Haddad, C. Wilson, A. Price, R. Emsley, G. Peat, M. Snow, M. Campbell, T. Howell, H. Johnson, S. McDonnell, T. Pinkney, M. Williams, H. Campbell, J. Davies, J. Li, C. Bagg, L. Haywood, A. Nicholson, J. Riches, S. Symons, M. Vertue, L. Al Mouazzen, R. Bray, D. Clark, J. Coulthard, T. Holland, N. Howells, A. Jones, R. Kapur, A. Kiszely, H. Krishnan, K. MacDonald-Taylor, J. Manara, J. Murray, C. Negrut, V. Pai, A. Porteous, S. Putnis, J. Robinson, S. Rupasinghe, V. Selvaratnam, J. Smith, N. Smith, J. Stevens, C. Taylor, A. Theodorides, N. Vetharajan, H. Vint, L. Young, S. Bullock, R. Cook, A. Dodds, A. Freeman-Hicks, P. Hillout, T. Cornell, A. Coutts, S. Dean, N. Devooght-Johnson, E. Ferrell, E. Fletcher, C. Hall, B. Kent, S. Kessly, R. Kincaid, M. Lazizi, A. Mostafa, T. Nisbett, T. Powell, P. Riddlestone, A. Roberton, J. Summers, L. Whitbread, B. Wroath, E. Fenlon, A. Hall, H. Jeffrey, R. Thonse, D. Dunne, A. Metcalfe, K. McGowan, S. Middleton, F. Shah, T. Spalding, C. Marie Suddens, T. Sweed, J. Teuke, P. Thompson, D. Wright, J. Amero, E. Brown, H. Chissell, A. Croucher, G. Dickinson, C. Hawkes-Blackburn, A. Peacocke, G. Smith, C. Snipe, K. Dearnley, R. Mayahi, B. Andrews, M. Barcelona, H. Giles, A. Gokturk,

P. Harnett, K. Jeeves, J. Kadunyi, S. Mendoza, I. Reichert, M. Santamaria, H. Virdee, S. Anand, N. Aslam-Pervez, S. Draycott, F. Howarth, I. Jina, N. Maher, D. Ross, L. Worstenholme, A. Baig, A. Bhaskaran, D. Banks, T. Brear, C. Christie, L. Cowen, J. Davis, R. Dixey, C. Esler, A. Essop-Adam, C. Haines, L. Houchen-Wolloff, H. Varachia, R. Wood, G. Gray, J. Nichols, A. Panes, S. Partridge, L. Rogerson, P. Sharma, D. Triggs, I. Venables, D. Wilcock, S. Buckley, T. Darian, E. Denis, J. Duncan, C. Hirst, J. Newman, F. Richardson, J. Smith, M. Adcode, M. Cottingham, E. Foster, A. Kelly, N. McKay, J. Rewbury, A. Whitcher, J. Williams, E. Zebracki, L. Davies, J. Jayachandran, A. Tardivel, V. Whitehead, M. Batting, A. Bond, M. Deakin, C. Dodd, A. Hudak, S. Hynes, L. Jones, G. Lang, D. McKenna, S. Morris, C. Scott-Dempster, A. Sykes, I. Vichos, S. Wood, R. Clifton, S. Diaz, C. Hendy, N. Modi, B. O'Mahony, S. O'Sullivan, N. Parker, M. Pecheva, R. Rumonovic, E. McLoughlin, J. Rushbrook, A. Thornhill, V. Parkinson, R. Sales, K. Van De Snepscheut-Jones, D. Wilcock, D. Wright, J. Allison, S. Baker, K. Beesley, G. Ferrari, B. Lankester, A. Lewis, J. Lyons, J. O'Callaghan, S. Sutcliffe, D. Wood, E. Bannister, C. Brown, D. Burden, T. Campbell, E. Craig, R. Easow, J. Foxton, A. Hazlerigg, C. Jayabev, R. Murdoch, G. Parsons, H. Brown, P. Carvelli, R. Montaser, A. Pepper, S. Sivarajan, O. Templeton-Ward, E. Wilson, J. Cronin, S. Diment, V. King, K. Shean, L. Vachtsevanos, K. Wilcocks, B. Wilson, P. McNestry, J. Ollerenshaw, J. Stoddard, P. Sutton, S. Anand, J. Bell, A. Chikate, D. Daniel, T. Davies, T. Finnigan, A. Frasquet-Garcia, S. Hopkins, S. Kerrison, A. McGowan, D. Sands Johnson, L. Smith, P. Turner, H. Wilkinson, L. Allsop, D. Anthony, R. Boulton, S. Brown, V. Desai, M. Gill, C. Heeley, S. Kulkarni, W. Lovegrove, D. Nash, T. Ann Sewell, S. Shelton, K. Slack, J. Cartwright, L. Connor, A. Davies, C. Davies, G. Gainard, D. Graham-Woollard, C. Murphy, L. Quinn, C. Thomas, J. Travers, M. Williams, A. Bell, S. Deo, K. Francis, T. Jackson, L. McCafferty, B. Navadgi, K. Plank, V. Satish, C. Thelwall, R. Knight, R. Patel, B. Paton, A. Acharya, U. Aland, M. Areirobulos, P. de Feyter, L. Ditchfield, H. Iqbaz, D. Massey, G. Stables, S. Appleby, M. Brown, S. Cable, A. Damen, J. Da Rocha, L. Foster, E. Hamilton, C. Hatton, C. Honeywell, K. Kulkarni, L. Markham, H. Mohammed, J. O'Grady, Y. Joshi, H. McLintock, T. Morgan, J. Stockport, V. Whitehead, P. Agrawal, J. Armstrong, S. Briggs, B. Coupe, A. Evans, R. Gilbert, S. Latham and A. Mohammed, *Lancet*, 2022, **400**, 605–615.

4 M. Reijman, V. Eggerding, E. van Es, E. van Arkel, I. van den Brand, J. van Linge, J. Zijl, E. Waarsing, S. Bierma-Zeinstra and D. Meuffels, *BMJ*, 2021, **372**, n375.

5 R. James, G. Kesturu, G. Balian and A. B. Chhabra, *J. Hand Surg.*, 2008, **33**, 102–112.

6 V. Musahl and J. Karlsson, *N. Engl. J. Med.*, 2019, **380**, 2341–2348.

7 T. Khan, A. Alvand, D. Prieto-Alhambra, D. J. Culliford, A. Judge, W. F. Jackson, B. E. Scammell, N. K. Arden and A. J. Price, *Br. J. Sports Med.*, 2019, **53**, 965–968.

8 S. G. Abram, A. J. Price, A. Judge and D. J. Beard, *Br. J. Sports Med.*, 2020, **54**, 286–291.

9 F. H. Ayman Gabr, *The National Ligament Registry*, *The Seventh Annual Report* (2022), **https://www.uknlr.co.uk/pdf/annual-report-2022.pdf**, (accessed 04 December, 2024).

10 A. P. Monk, L. J. Davies, S. Hopewell, K. Harris, D. J. Beard and A. J. Price, *Cochrane Database Syst. Rev.*, 2016, 1–30.

11 B. L. van Meer, D. E. Meuffels, W. A. van Eijsden, J. A. N. Verhaar, S. M. A. Bierma-Zeinstra and M. Reijman, *Br. J. Sports Med.*, 2015, **49**, 975–983.

12 S. R. Filbay, M. Dowsett, M. Chaker Jomaa, J. Rooney, R. Sabharwal, P. Lucas, A. Van Den Heever, J. Kazaglis, J. Merlino, M. Moran, M. Allwright, D. E. K. Kuah, R. Durie, G. Roger, M. Cross and T. Cross, *Br. J. Sports Med.*, 2023, **57**, 1490–1497.

13 R. Lanza, R. Langer, J. P. Vacanti and A. Atala, *Principles of tissue engineering*, Academic press, 2020.

14 S. Chen, J. Wang, Y. Chen, X. Mo and C. Fan, *Mater. Sci. Eng. C*, 2021, **119**, 111506.

15 D. Perry and M. O'Connell, *Osteopath. Fam. Physician*, 2015, 7.

16 H. J. Silvers and B. R. Mandelbaum, *Sport-Orthopädie-Sport-Traumatologie-Sports Orthopaedics and Traumatology*, 2011, vol. 27, pp. 18–26.

17 J. P. van der List, *Br. J. Sports Med.*, 2022, **56**, 1053–1054.

18 V. Musahl, I. D. Engler, E. M. Nazzal, J. F. Dalton, G. A. Lucidi, J. D. Hughes, S. Zaffagnini, F. Della Villa, J. J. Irrgang and F. H. Fu, *Knee Surg. Sports Traumatol. Arthrosc.*, 2022, 1–18.

19 L. Pang, P. Li, T. Li, Y. Li, J. Zhu and X. Tang, *Front. Surg.*, 2022, **9**, 887522.

20 J. A. Feagin, C. M. Pierce and M. R. Geyer, *The ACL-deficient knee*, Springer, 2013, pp. 97–104.

21 E. M. Magarian, B. C. Fleming, S. L. Harrison, A. N. Mastrangelo, G. J. Badger and M. M. Murray, *Am. J. Sports Med.*, 2010, **38**, 2528–2534.

22 R. E. Boykin, W. G. Rodkey and J. R. Steadman, *The ACL-Deficient Knee*, Springer, 2013, pp. 203–210.

23 K. Samuelsson, D. Andersson, M. Ahldén, F. H. Fu, V. Musahl and J. Karlsson, *Clin. Sports Med.*, 2013, **32**, 111–126.

24 T. W. Lin, L. Cardenas and L. J. Soslowsky, *J. Biomech.*, 2004, **37**, 865–877.

25 M. M. Murray, R. Bennett, X. Zhang and M. Spector, *J. Orthop. Res.*, 2002, **20**, 875–880.

26 M. M. Murray and M. Spector, *Biomaterials*, 2001, **22**, 2393–2402.

27 A. Gobbi, L. Boldrini, G. Karnatzikos and V. Mahajan, *Sports Injuries*, Springer, 2012, pp. 475–484.

28 N. K. Paschos and H. S. Vasiliadis, *Cochrane Database Syst. Rev.*, 2018, **2018**, CD010661.

29 K. B. Freedman, M. J. D'Amato, D. D. Nedeff, A. Kaz and B. R. Bach, *Am. J. Sports Med.*, 2003, **31**, 2–11.

30 T. E. Foster, B. L. Wolfe, S. Ryan, L. Silvestri and E. Krall Kaye, *Am. J. Sports Med.*, 2010, **38**, 189–199.

31 P. Ducheyne, *Comprehensive biomaterials*, Elsevier, 2015.

32 A. Weiler, C. Förster, P. Hunt, R. Falk, T. Jung, F. N. Unterhauser, V. Bergmann, G. Schmidmaier and N. P. Haas, *Am. J. Sports Med.*, 2004, **32**, 881–891.
33 D. Hart, T. Gurney-Dunlop, J. Leiter, R. Longstaffe, A. S. Eid, S. McRae and P. MacDonald, *Eur. J. Orthop. Surg. Traumatol.*, 2023, **33**, 1067–1074.
34 M. Laranjeira, R. M. Domingues, R. Costa-Almeida, R. L. Reis and M. E. Gomes, *Small*, 2017, **13**, 1700689.
35 L. Wang, F. Wan, Y. Xu, S. Xie, T. Zhao, F. Zhang, H. Yang, J. Zhu, J. Gao and X. Shi, *Nat. Nanotechnol.*, 2023, 1–9.
36 B. Aghaei-Ghareh-Bolagh, S. M. Mithieux, M. A. Hiob, Y. Wang, A. Chong and A. S. Weiss, *Acta Biomater.*, 2019, **91**, 112–122.
37 G. Yang, H. Lin, B. B. Rothrauff, S. Yu and R. S. Tuan, *Acta Biomater.*, 2016, **35**, 68–76.
38 B. B. Rothrauff, B. B. Lauro, G. Yang, R. E. Debski, V. Musahl and R. S. Tuan, *Tissue Eng., Part A*, 2017, **23**, 378–389.
39 A. Jayasree, S. Kottappally Thankappan, R. Ramachandran, M. N. Sundaram, C.-H. Chen, U. Mony, J.-P. Chen and R. Jayakumar, *ACS Biomater. Sci. Eng.*, 2019, **5**, 1476–1486.
40 M. M. Murray, B. C. Fleming, G. J. Badger, B. T. Team, C. Freiberger, R. Henderson, S. Barnett, A. Kiapour, K. Ecklund and B. Proffen, *Am. J. Sports Med.*, 2020, **48**, 1305–1315.
41 C. Legnani and A. Ventura, *Med. Eng. Phys.*, 2023, **117**, 103992.
42 P. Mahapatra, S. Horriat and B. S. Anand, *J. Exp. Orthop.*, 2018, **5**, 20.
43 H. Gao, L. Sun, C. Yu, M. Huang, S. Feng, D. Sheng, M. Tim Yun Ong, F. Sai Chuen Bruma, X. Yang, Y. Hao, C. Rolf, S. Chen, Y. Li and J. Chen, *Am. J. Sports Med.*, 2025, **53**, 1347–1358.
44 L. M. Batty, C. J. Norsworthy, N. J. Lash, J. Wasiak, A. K. Richmond and J. A. Feller, *Arthroscopy*, 2015, **31**, 957–968.
45 J. R. Ebert and P. T. Annear, *Orthop. J. Sports Med.*, 2019, **7**, 2325967119879079.
46 T. M. Tiefenboeck, E. Thurmaier, M. M. Tiefenboeck, R. C. Ostermann, J. Joestl, M. Winnisch, M. Schurz, S. Hajdu and M. Hofbauer, *Knee*, 2015, **22**, 565–568.
47 M. A. Smolle, S. F. Fischerauer, S. Zötsch, A. V. Kiegerl, P. Sadoghi, G. Gruber, A. Leithner and G. A. Bernhardt, *Bone Joint J.*, 2022, **104**, 242–248.
48 S. J. Tulloch, B. M. Devitt, T. Porter, T. Hartwig, H. Klemm, S. Hookway and C. J. Norsworthy, *Knee Surg. Sports Traumatol. Arthrosc.*, 2019, **27**, 3626–3632.
49 J. Huang, M. Wu, Q. Huang, T. Yang, G. Zhao and P. Ma, *J. Ind. Text.*, 2024, **54**, 15280837241280402.
50 K. Sindhi, R. B. Pingili, V. Beldar, S. Bhattacharya, J. Rahaman and D. Mukherjee, *J. Tissue Viability*, 2025, **34**, 100858.
51 D. Figueroa, M. Espinosa, R. Calvo, M. Scheu, A. Vaisman, M. Gallegos and P. Conget, *Knee Surg. Sports Traumatol. Arthrosc.*, 2014, **22**, 1196–1202.
52 A. Teuschl, P. Heimel, S. Nürnberger, M. Van Griensven, H. Redl and T. Nau, *Am. J. Sports Med.*, 2016, **44**, 1547–1557.
53 H. Fan, H. Liu, E. J. W. Wong, S. L. Toh and J. C. H. Goh, *Biomaterials*, 2008, **29**, 3324–3337.
54 M. S. Peach, S. G. Kumbar, R. James, U. S. Toti, D. Balasubramaniam, M. Deng, B. Ulery, A. D. Mazzocca, M. B. McCarthy and N. L. Morozowich, *J. Biomed. Nanotechnol.*, 2012, **8**, 107–124.
55 P. Buma, H. Kok, L. Blankevoort, W. Kuijpers, R. Huiskes and A. Van Kampen, *Int. Orthop.*, 2004, **28**, 91–96.
56 N. L. Leong, F. A. Petrigliano and D. R. McAllister, *J. Biomed. Mater. Res., Part A*, 2014, **102**, 1614–1624.
57 H. H. Lu, J. A. Cooper Jr, S. Manuel, J. W. Freeman, M. A. Attawia, F. K. Ko and C. T. Laurencin, *Biomaterials*, 2005, **26**, 4805–4816.
58 R. James, U. S. Toti, C. T. Laurencin and S. G. Kumbar, *Biomedical nanotechnology*, Springer, 2011, pp. 243–258.
59 J. A. Cooper, J. S. Sahota, W. J. Gorum, J. Carter, S. B. Doty and C. T. Laurencin, *Proc. Natl. Acad. Sci. U. S. A.*, 2007, **104**, 3049–3054.
60 M. Gwiazda, S. Kumar, W. Świeszkowski, S. Ivanovski and C. Vaquette, *J. Mech. Behav. Biomed. Mater.*, 2020, **104**, 103631.
61 D. A. Brennan, A. A. Conte, G. Kanski, S. Turkula, X. Hu, M. T. Kleiner and V. Beachley, *Adv. Healthcare Mater.*, 2018, **7**, 1701277.
62 N. L. Leong, N. Kabir, A. Arshi, A. Nazemi, J. Jiang, B. M. Wu, F. A. Petrigliano and D. R. McAllister, *J. Orthop. Res.*, 2016, **34**, 828–835.
63 F. Bi, Y. Chen, J. Liu, Y. Wang, D. Xu and K. Tian, *J. Orthop. Surg. Res.*, 2021, **16**, 139.
64 M. C. Bonferoni, C. Caramella, L. Catenacci, B. Conti, R. Dorati, F. Ferrari, I. Genta, T. Modena, S. Perteghella and S. Rossi, *Pharmaceutics*, 2021, **13**, 1341.
65 S. Liu, A. Al-Danakh, H. Wang, Y. Sun and L. Wang, *Biotechnol. J.*, 2024, **19**, 2300251.
66 X. Xie, X. Wang, D. Ding, C. Li, J. Li, J. Lin, F. Wang and L. Wang, *Nano Today*, 2024, **56**, 102277.
67 J. Li, C. Xue, H. Wang, S. Dong, Z. Yang, Y. Cao, B. Zhao, B. Cheng, X. Xie and X. Mo, *Small*, 2022, **18**, 2201147.
68 M. S. Mazzeo, T. Chai, M. Daviran and K. M. Schultz, *ACS Appl. Bio Mater.*, 2018, **2**, 81–92.
69 J. F. Jameson, M. O. Pacheco, J. E. Butler and W. L. Stoppel, *Front. Bioeng. Biotechnol.*, 2021, **9**, 664306.
70 H. Shui, Q. Shi, N. M. Pugno, Q. Chen and Z. Li, *J. Mech. Behav. Biomed. Mater.*, 2019, **96**, 324–333.
71 E. Batoni, A. F. Bonatti, C. De Maria, K. Dalgarno, R. Naseem, U. Dianzani, C. L. Gigliotti, E. Boggio and G. Vozzi, *Pharmaceutics*, 2023, **15**, 815.
72 J. Cai, J. Liu, J. Xu, Y. Li, T. Zheng, T. Zhang, K. Han, S. Chen, J. Jiang and S. Wu, *Biofabrication*, 2023, **15**, 025002.
73 T. Gereke, O. Döbrich, D. Aibibu, J. Nowotny and C. Cherif, *J. Ind. Text.*, 2017, **47**, 408–425.
74 P. Y. Mengsteab, J. Freeman, M. A. Barajaa, L. S. Nair and C. T. Laurencin, *Regener. Eng. Transl. Med.*, 2021, **7**, 524–532.
75 G. Giavaresi, M. Sartori, M. Baleani, S. Brogini, P. Erani, D. Dallari, N. Del Piccolo, C. E. Ghezzi, L. Martini,

A. Parrilli, A. Boschi, M. C. Tanzi, A. Alessandrino, M. Fini, G. Freddi and S. Farè, *Biomater. Adv.*, 2025, **166**, 214029.
76 Z. Zheng, J. Ran, W. Chen, Y. Hu, T. Zhu, X. Chen, Z. Yin, B. C. Heng, G. Feng and H. Le, *Acta Biomater.*, 2017, **51**, 317–329.
77 R. D. Smith, N. Zargar, C. P. Brown, N. S. Nagra, S. G. Dakin, S. J. Snelling, O. Hakimi and A. Carr, *J. Shoulder Elb. Surg.*, 2017, **26**, 2038–2046.
78 S. L.-Y. Woo, J. M. Hollis, D. J. Adams, R. M. Lyon and S. Takai, *Am. J. Sports Med.*, 1991, **19**, 217–225.
79 S. Elmarzougui, S. Ben Abdessalem and F. Sakli, *J. Text. Inst.*, 2010, **101**, 788–794.
80 F. Noyes and E. Grood, *J Bone Joint Surg Am*, 1976, **58**, 1074–1082.
81 M. Marieswaran, I. Jain, B. Garg, V. Sharma and D. Kalyanasundaram, *Appl. Bionics Biomech.*, 2018, **2018**, 4657824.
82 M. Rittmeister, P. C. Noble, D. M. Lintner, J. W. Alexander, M. Conditt and H. W. Kohl III, *Arthroscopy*, 2002, **18**, 194–200.
83 H. Matsumoto and K. Fujikawa, *Keio J. Med.*, 2001, **50**, 161–166.
84 C. Legnani, A. Ventura, C. Terzaghi, E. Borgo and W. Albisetti, *Int. Orthop.*, 2010, **34**, 465–471.
85 H. Jedda, S. B. Abessalem and F. Sakli, *J. Text. Inst.*, 2011, **102**, 332–342.
86 A. Sensini, C. Gotti, J. Belcari, A. Zucchelli, M. L. Focarete, C. Gualandi, I. Todaro, A. P. Kao, G. Tozzi and L. Cristofolini, *Med. Eng. Phys.*, 2019, **71**, 79–90.
87 C. Aka and G. Basal, *J. Mech. Behav. Biomed. Mater.*, 2022, **126**, 105063.
88 L. Savić, E. M. Augustyniak, A. Kastensson, S. Snelling, R. E. Abhari, M. Baldwin, A. Price, W. Jackson, A. Carr and P.-A. Mouthuy, *Mater. Sci. Eng.: C*, 2021, **129**, 112414.
89 N. L. Leong, N. Kabir, A. Arshi, A. Nazemi, B. Wu, F. A. Petrigliano and D. R. McAllister, *Tissue Eng., Part A*, 2015, **21**, 1859–1868.
90 C. Liu, J. Dai, X. Wang and X. Hu, *Polymers*, 2023, **15**, 3003.
91 L. Suamte and P. J. Babu, *Nano TransMed.*, 2024, 100055.
92 Y. Chen, X. Dong, M. Shafiq, G. Myles, N. Radacsi and X. Mo, *Adv. Fiber Mater.*, 2022, **4**, 959–986.
93 Y. Gao, W. Shao, W. Qian, J. He, Y. Zhou, K. Qi, L. Wang, S. Cui and R. Wang, *Mater. Sci. Eng.: C*, 2018, **84**, 195–207.
94 X. Xie, J. Cai, Y. Yao, Y. Chen, J. Wu and X. Mo, *Composites, Part B*, 2021, **212**, 108679.
95 W. Shao, J. He, Q. Han, F. Sang, Q. Wang, L. Chen, S. Cui and B. Ding, *Mater. Sci. Eng.: C*, 2016, **67**, 599–610.
96 Y. Wu, L. Wang, B. Guo and P. X. Ma, *ACS Nano*, 2017, **11**, 5646–5659.
97 M. Younesi, A. Islam, V. Kishore, J. M. Anderson and O. Akkus, *Adv. Funct. Mater.*, 2014, **24**, 5762–5770.
98 J. L. Ng, L. E. Knothe, R. M. Whan, U. Knothe and M. L. K. Tate, *Sci. Rep.*, 2017, **7**, 40396.
99 G. Roudier, M. Hourques, N. Da Silva, M. Gluais, E. Binyet, J.-M. Olive and N. L'heureux, *Biofabrication*, 2023, **16**, 015015.
100 L. Magnan, G. Labrunie, M. Fénelon, N. Dusserre, M.-P. Foulc, M. Lafourcade, I. Svahn, E. Gontier, T. N. Mcallister and N. L'Heureux, *Acta Biomater.*, 2020, **105**, 111–120.
101 F. Schäfer-Nolte, K. Hennecke, K. Reimers, R. Schnabel, C. Allmeling, P. M. Vogt, J. W. Kuhbier and U. Mirastschijski, *Ann. Surg.*, 2014, **259**, 781–792.
102 S. Wu, Y. Wang, P. N. Streubel and B. Duan, *Acta Biomater.*, 2017, **62**, 102–115.
103 K. Grömer, *The Art of Prehistoric Textile Making: The development of craft traditions and clothing in Central Europe*, Naturhistorisches Museum Wien, 2016.
104 X. Gong, X. Chen and Y. Zhou, *High-Performance Apparel*, Elsevier, 2018, pp. 75–112.
105 C. Bessette, M. Decrette, M. Tourlonias, J.-F. Osselin, F. Charleux, D. Coupé and M.-A. Bueno, *Composites, Part A*, 2019, **126**, 105604.
106 T. Yoshida, *Text. Res. J.*, 2023, **93**, 3527–3537.
107 J. Hu, *3D Fibrous Assemblies*, ed J. Hu, Woodhead Publishing, 2008, pp. 104–130.
108 A. A. Almetwally and M. Mourad, *J. Text. Inst.*, 2014, **105**, 235–245.
109 I. Jahan, *Adv. Res. Text. Eng.*, 2017, **2**, 1018.
110 K. Bircher, M. Zündel, M. Pensalfini, A. E. Ehret and E. Mazza, *Nat. Commun.*, 2019, **10**, 792.
111 A. Liberski, N. Ayad, D. Wojciechowska, R. Kot, D. M. Vo, D. Aibibu, G. Hoffmann, C. Cherif, K. Grobelny-Mayer and M. Snycerski, *Biotechnol. Adv.*, 2017, **35**, 633–656.
112 C. Norberg, G. Filippone, F. Andreopoulos, T. M. Best, M. Baraga, A. R. Jackson and F. Travascio, *J. Biomech.*, 2021, **120**, 110343.
113 Y. S. Perera, R. M. H. W. Muwanwella, P. R. Fernando, S. K. Fernando and T. S. S. Jayawardana, *Fashion Text.*, 2021, **8**, 1–31.
114 J. R. Duflou, Y. Deng, K. Van Acker and W. Dewulf, *MRS Bull.*, 2012, **37**, 374–382.
115 X. Chen and D. Sun, *Prof Yao Mu 80th Birthday Celebrations and Advanced International Textile*, 2009, 1–24.
116 S. Eriksson and L. Sandsjö, *Advances in 3D textiles*, Elsevier, 2015, pp. 305–340.
117 X. Chen, L. W. Taylor and L.-J. Tsai, *Text. Res. J.*, 2011, **81**, 932–944.
118 T. G. Lang, D. Nuß, T. Gereke, G. Hoffmann, M. Wöltje, D. Aibibu and C. Cherif, *Textiles*, 2022, **2**, 336–348.
119 J. Gilmore, F. Yin and K. J. Burg, *J. Biomed. Mater. Res., Part B*, 2019, **107**, 306–313.
120 X. Sun, L. Tong, M. D. Wood and Y.-W. Mai, *Compos. Sci. Technol.*, 2004, **64**, 967–981.
121 E. Cukierman, R. Pankov, D. R. Stevens and K. M. Yamada, *Science*, 2001, **294**, 1708–1712.
122 G. D. Learn, P. E. McClellan, D. M. Knapik, J. L. Cumsky, V. Webster-Wood, J. M. Anderson, R. J. Gillespie and O. Akkus, *J. Biomed. Mater. Res., Part B*, 2019, **107**, 1864–1876.
123 M. Kapałczyńska, T. Kolenda, W. Przybyła, M. Zajączkowska, A. Teresiak, V. Filas, M. Ibbs, R. Bliźniak, Ł. Łuczewski and K. Lamperska, *Arch. Med. Sci.*, 2018, **14**, 910–919.
124 J. Lee, M. J. Cuddihy and N. A. Kotov, *Tissue Eng., Part B*, 2008, **14**, 61–86.

125 M. Lee, *Tissue Eng., Part B*, 2008, **14**, 61.
126 M. Zietarska, C. M. Maugard, A. Filali-Mouhim, M. Alam-Fahmy, P. N. Tonin, D. M. Provencher and A. M. Mes-Masson, *Molecular Carcinogenesis: Published in cooperation with the University of Texas MD Anderson Cancer Center*, 2007, vol. 46, pp. 872–885.
127 L. Huang, J. Huang, H. Shao, X. Hu, C. Cao, S. Fan, L. Song and Y. Zhang, *Mater. Sci. Eng.: C*, 2019, **94**, 179–189.
128 M. S. Islam, B. C. Ang, A. Andriyana and A. M. Afifi, *SN Appl. Sci.*, 2019, **1**, 1–16.
129 C. M. Murphy, G. P. Duffy, A. Schindeler and F. J. O'brien, *J. Biomed. Mater. Res., Part A*, 2016, **104**, 291–304.
130 C. M. Murphy, M. G. Haugh and F. J. O'brien, *Biomaterials*, 2010, **31**, 461–466.
131 F. J. O'Brien, B. Harley, I. V. Yannas and L. J. Gibson, *Biomaterials*, 2005, **26**, 433–441.
132 G. Bahcecioglu, N. Hasirci and V. Hasirci, *Biomed. Mater.*, 2018, **13**, 035005.
133 M. Chen, P. K. Patra, S. B. Warner and S. Bhowmick, *Tissue Eng.*, 2007, **13**, 579–587.
134 Y. Jiao, C. Li, L. Liu, F. Wang, X. Liu, J. Mao and L. Wang, *Biomater. Sci.*, 2020, **8**, 3574–3600.
135 P. Feng, J. He, S. Peng, C. Gao, Z. Zhao, S. Xiong and C. Shuai, *Mater. Sci. Eng.: C*, 2019, **100**, 809–825.
136 C. Xie, Q. Gao, P. Wang, L. Shao, H. Yuan, J. Fu, W. Chen and Y. He, *Mater. Des.*, 2019, **181**, 108092.
137 T. L. Jenkins and D. Little, *npj Regener. Med.*, 2019, **4**, 15.
138 N. Abbasi, S. Hamlet, R. M. Love and N.-T. Nguyen, *J. Sci. Adv. Mater. Dev.*, 2020, **5**, 1–9.
139 Q. L. Loh and C. Choong, *Tissue Eng., Part B*, 2013, **19**(6), 485–502.
140 M. Rashid, J. Dudhia, S. G. Dakin, S. J. Snelling, R. De Godoy, P.-A. Mouthuy, R. K. Smith, M. Morrey and A. J. Carr, *Sci. Rep.*, 2020, **10**, 4754.
141 C. Pereira-Lobato, M. Echeverry-Rendón, J. Fernández-Blázquez, C. González and J. LLorca, *J. Mech. Behav. Biomed. Mater.*, 2024, **150**, 106340.

